Uri Gat
72:056

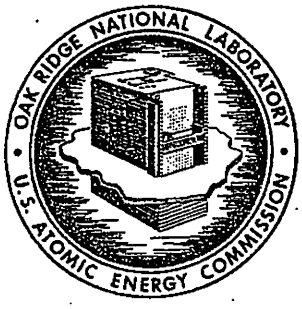

OAK RIDGE NATIONAL LABORATORY
OPERATED BY
UNION CARBIDE CORPORATION
NUCLEAR DIVISION
POST OFFICE BOX X
OAK RIDGE, TENNESSEE 37830

FOR INTERNAL USE ONLY

ORNL
CENTRAL FILES NUMBER
72 - 6 - 12

DATE: June 30, 1972

SUBJECT: SIDESTREAM PROCESSING FOR CONTINUOUS IODINE AND XENON REMOVAL FROM THE MSBR FUEL

TO: Distribution

FROM: R. P. Wichner
with C. F. Baes

ABSTRACT

An attempt is made to set forth what it would take to continuously remove iodine from the MSBR fuel by processing a sidestream of the primary flow. Although no final judgment as to the ultimate desirability of stripping iodine can be made until further experiments and evaluation are undertaken, the conclusion is reached that available evidence indicates this to be a reasonable developmental goal pending satisfactory resolution of uncertainties in the following areas: (1) Verification is needed regarding the degree of separation that can be achieved by various types of contactors. (2) What has been assumed regarding the chemistry of iodine stripping needs to be verified on a laboratory scale using a chemical environment that closely represents actual conditions. (3) A determination must be made on how oxidizing localized portions of the primary system may be permitted to become.

In Chapter 2 a discussion is presented on the chemistry of iodine stripping from fuel salt. Some rather speculative designs of four types of iodine stripping units are presented in Chapter 3.

KEYWORDS: Holdup, Iodides, Iodines, MSBR, Sparging, Sprays, Volatility, Xenon

CONTENTS

SUMMARY

This report attempts to set forth what it would take to continuously remove iodine from the MSBR fuel by processing a sidestream of the primary flow. The greatest benefit for iodine stripping is attained when it is assumed that impervious graphite coatings are not available. In this case xenon moves into the graphite with such speed that there is a particularly high incentive to capture the mass-135 fission product before it decays to xenon. Throughout this report the graphite is assumed to be uncoated and similar to that used in the MSRE.

The two basic approaches to the problem of iodine removal are presented in Chapter 1. First, one may consider a contactor intended for iodine stripping alone. This has the virtue of requiring only small bypass flows (about 0.8% of the primary flow) and reasonably small equipment size. The disadvantage is that the target xenon poison level cannot be achieved solely by this means — although the iodine stripper would capture about 80% of the mass-135 poison, additional xenon removal provisions must be made to reduce the poison fraction to 1/2% δk/k.

The second approach is to use higher bypass flows in order to capture sufficient xenon along with the iodine so that no additional control measures are needed. With uncoated graphite this may be accomplished with bypass flows of about 8% of the primary flow. This latter approach was favored at the outset of this work, however, after developing some flowsheets and contactor designs for the two methods it is now thought that iodine stripping alone is the preferred method.

A preliminary flowsheet for iodine removal alone is shown in Fig. 9. The stripping gas flow rate is 80 cfs of helium containing 0.01 atm HF, which oxidizes the fuel salt from an assumed U^{+4}/U^{+3} ratio of 10^4 to 3×10^6 at the exit of the stripping unit. Thus, HF is consumed at a rate of 0.01 ℓSTP/sec. The salt is returned to its original state by addition of reductant. Figure 9 shows a reductant addition rate of 5.0, 1.5, and 29.2 g/hr of Li°, Be°, and Th°, respectively, which must ultimately be removed by the chemplant. This manner of adding reductant is shown because it leaves unaltered the molar ratios of Li, Be, and Th in the fuel.

However, the text notes that 7.6 and 2.2 g/hr of Li° and Be° could be added instead with the intention of leaving it in the fuel. This would alter the fuel composition, but probably at an acceptably slow rate.

In Chapter 2 the chemistry of iodine removal from MSBR fuel is discussed. Emphasis is placed on full understanding of available laboratory data on iodine stripping from lithium-beryllium fluoride melts. The apparently anomolous behavior of these data is explained by assuming the stripping rate to be controlled by I^- diffusion to the gas/liquid interface. It is shown that this assumption accurately accounts for the observed variation of the apparent equilibrium constant with HF partial pressure as well as observed trends of the stripping rate with temperature and mole fraction Be^{++}.

The chemical environment in an MSBR iodine stripper would differ significantly from that which existed in the laboratory experiments — the stripping gas would be primarily helium rather than hydrogen, iodine concentrations would be about 20,000 times lower, and the presence of the U^{+3}/U^{+4} couple offers an additional complication. Despite these differences it is felt that iodine stripping from MSBR fuel is understood well enough to allow some speculation on the design of practical stripper units.

Four types of contactors are examined in Chapter 3 for use as iodine strippers or for combined xenon and iodine removal. It is shown that for either case the required number of transfer units of separation is reasonably small so that efficiency of separation is not an important factor in the selection of the type of contactor. All the four contactors considered are probably worthy of further examination, however, the spray desorber appears at this time to be the best choice. Here we speak of a device in which the separation is accomplished in the spray zone near the nozzle rather than the much larger, conventional spray tower where the bulk of the separation is presumed to occur from quiescently falling drops. The spray desorber offers the advantage of small size and low liquid holdup. If conditions at the inlet nozzle prove to be too severe, the venturi scrubber may be a good alternative that requires less demanding inlet conditions.

The two other types of contactors considered are the so-called "ramp stripper" and the packed column. The ramp stripper offers the possibility of effecting the liquid/gas contact in a relatively calm, closely regulated countercurrent fashion that could be a highly desirable feature, for example, if foaming were a problem in the spray devices. However, the value of the mass transfer coefficient in this device is highly uncertain and needs to be experimentally verified. Packed columns are presently limited by low measured values of the effective mass transfer coefficient. This is partly caused by the nonwetting character of the fuel salt, which results in a low liquid surface area within the column. Thus packed columns tend to be rather large, but within the realm of possibility for iodine stripping alone.

RECOMMENDATIONS

1. The laboratory experiments on iodine stripping from lithium-beryllium fluoride melts should be repeated using conditions that more closely approach those expected in an MSBR contactor. As a minimum, the carrier gas should be helium instead of hydrogen, the iodine concentration should be reduced to anticipated levels, and uranium added to the melt. If possible, counterflow film contact should be used so that accurate mass transfer data as well as chemical equilibria may be obtained.

2. Iodine stripping experiments should be designed for the Gas System Test Facility. These could include:

   a. determination of the number of transfer units of iodine and xenon separation obtained by spray desorption, and

   b. determination of the mass transfer coefficient in a counterflow contactor such as the ramp stripper. Means for elevating the transfer rate by roughness elements should be tried.

3. Some attempt should be made to determine what effective mass transfer coefficients may reasonably be expected in a packed column iodine stripper. Present tests of these devices indicate rather low values for k_L, which, however, appear to be satisfactory for the intended use in the Chemical Processing Facility. Values for k_L in a packed tower may be

elevated by

a. selecting a larger diameter column for test to reduce the fraction of liquid that bypasses the packing by flowing down the wall, and

b. judicious selection of packing size and shape to maximize the exposed liquid contact surface in the column.

1. INTRODUCTION

In this report we consider the possibility of processing a sidestream of the primary flow of an MSBR for xenon or iodine removal. The required rate of sidestream processing to achieve a desired poison level depends on the rates of competing, undesirable processes. For the specie ^{135}I, through which 82% of the ^{135}Xe poison passes, the competing processes are diffusion into graphite and decay to xenon – burnup of ^{135}I being negligibly small. The chief attraction of iodine stripping lies in the fact that the competitive rates are quite low, and hence the major portion of the iodine could be captured by processing small sidestreams – in the range 0.2 to 0.4% of the primary flow or 120 to 240 gpm for a 100% efficient device.

The required iodine processing rate is determined principally by the rate of decay to xenon that occurs with a half-life of 6.7 hr. Evidence presented in Section 2.5 indicates that the iodine loss rate to the graphite pores – due both to vaporization of the volatile species LiI and BeFI and the desorption of HI and I – is negligibly small in comparison. In that circumstance it may be shown that the ratio of xenon concentration in the fuel with iodine being stripped with removal time T_I to that assuming no iodine stripping is given by,

$$\frac{[Xe]}{[Xe]_o} = Y_{Xe} + Y_I \left(\frac{1}{r+1}\right), \qquad (1)$$

where

$[Xe]$ = ^{135}Xe concentration in fuel with I stripping,

$[Xe]_o$ = ^{135}Xe concentration in fuel without I stripping,

Y_{Xe}, Y_I = fraction of mass 135 yield that is directly Xe and I, respectively. $Y_{Xe} = 0.18$, $Y_I = 0.82$,

$r = 1/T_I\lambda_I$, dimensionless I removal rate,

T_I = iodine removal time,

λ_I = ^{135}I decay constant.

The significance of Eq. (1) may be noted by examination of Fig. 1. The top line, obtained from values calculated by R. J. Kedl, relates the anticipated ^{135}Xe poison levels for uncoated graphite as a function of the rate of xenon removal, assuming no simultaneous removal of iodine. It may be seen that the objective of 1/2% ^{135}Xe poison level cannot be attained with solely xenon stripping except by resorting to bypass flows in excess of 15% of the primary flow rate, which we will assume for the present to be an upper practical limit.

The three lower curves of Fig. 1, which were computed from the top curve and Eq. (1), pertain to the situation when iodine is simultaneously removed with efficiencies of 10, 20, and 100%. Thus the top curve pertains to the case where the stripping gas is inert,* and the required gas flow rate is small due to the low solubility of xenon in fuel salt. To attain some nonnegligible amount of iodine stripping, HF must be added to the stripping gas. Additionally, much greater gas flows are required to keep the partial pressures of HI(g) and I(g) sufficiently low. The point here is that any iodine stripper, however inefficient, is likely to quite efficiently remove xenon as well — which is the reason for presenting the relationship of ^{135}Xe poison level and bypass flow rate in the fashion shown in Fig. 1.

Referring to Fig. 1, note that 1/2% poison levels may be achieved with very modest bypass flow rates and only small required iodine removal efficiencies. For example, when the bypass flow rate is 5 1/2% of the primary flow and 100% efficient xenon removal is presumed, the 1/2% poison level is achieved with only 10% iodine removal efficiency for the stripper.

---

*Some iodine will come off even with inert stripping gas. See discussion in Section 2.4.

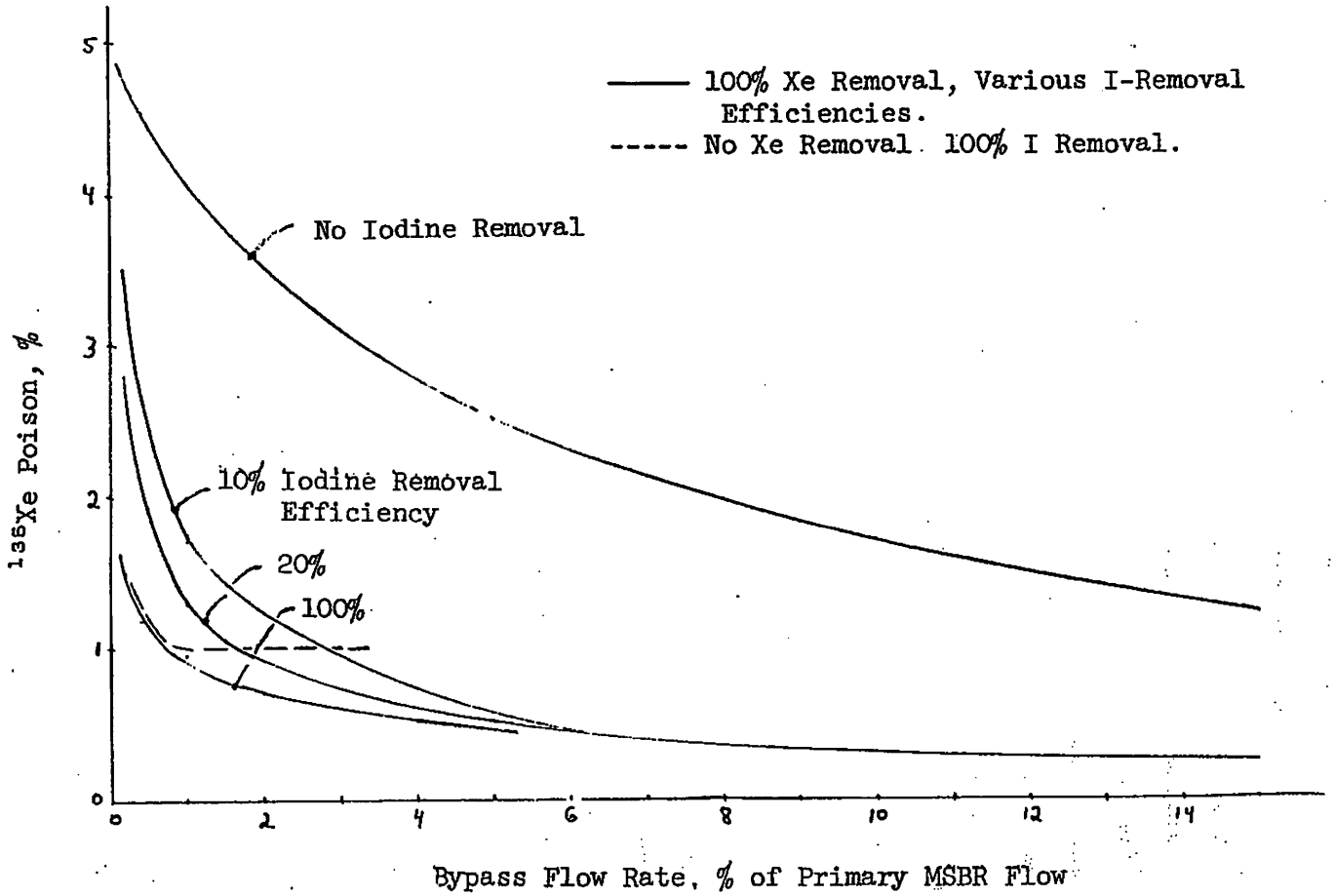

Fig. 1. ^{135}Xe Poison Fractions Using a Combined Xenon and Iodine Stripper (for Uncoated Graphite).

The dashed line shown in Fig. 1 relates the ^{135}Xe poison level to the bypass flow rate for the hypothetical situation of 100% iodine and no xenon removal. For this case there is a rapid reduction in xenon poison level with small increases in bypass flow rate. Essentially all the iodine is removed with about 0.8% bypass flow at which time the poison level approaches 1% – the value resulting from the ^{135}Xe direct yield. Comparison of the dashed curve with the solid line, which represents the case of 100% xenon and 100% iodine removal, indicates that with such low bypass flow, the amount of xenon removed is of small significance in reducing the ^{135}Xe poison level. Although iodine removal by itself is insufficient for achieving a 1/2% poison level, removal from small bypass flows can be extremely helpful to the attainment of such a goal.

Summarizing them:

1. Sidestream processing for xenon removal alone requires impractically high bypass flows unless some degree of graphite sealing is assumed to be available.

2. We may think in terms of a low bypass flow device designed solely for iodine removal that would supplement some other ^{135}Xe control system. In Section 3 we consider a stripper designed specifically for 0.8% bypass flow and 60% iodine removal efficiency which would capture about 80% of the MSBR ^{135}Xe production.

3. We could consider a larger flow-rate device designed for a reasonably high xenon-removal efficiency and a low but significant iodine-removal efficiency. In Section 3 the case of 8% bypass flow, 63% xenon removal, and 6.3% iodine removal is examined. Such flows and stripping efficiencies would result in a 1/2% ^{135}Xe poison level with no additional control measures.

It may be worthwhile at this time to itemize as carefully as possible the advantages and the disadvantages of sidestream processing for control of ^{135}Xe poison fraction.

1.1 Advantages of Sidestream Processing

1.1.1 Piping Simplicity

One process flow replaces the four parallel gas-separator loops of the present reference design.

1.1.2 Hydraulic Simplicity

Hydraulic transients are far simpler to analyze with only one bypass line instead of four; hence, prediction of off-design events are more certain. From a hydraulics point of view, the flow through a stripper is well understood compared with the relatively unknown dynamics of the vortex-flow gas separator.

1.1.3 Use of Standard Unit Operations

There is some advantage in employing standard separation devices as opposed to unique methods that are rarely used. Unique procedures, such as bubble circulation and vortex gas separation, have either been rejected in past commercial systems for some valid reason or may lead to unanticipated future difficulties.

1.1.4 Potential for Improvement

There are four types of stripping devices considered in this report, each one of which has a spectrum of design parameters that may be adjusted to improve contactor efficiency or diminish liquid holdup. In contrast, the characteristics of the circulating bubble system are largely inherent features that depend on noncontrollable surface properties or bubble dynamics.

1.1.5 Potential for Multiple Use

This is probably the greatest single advantage for sidestream processing. As knowledge expands on the behavior and disposition of fission products in the fuel salt, means may become evident to advantageously use a sidestream iodine or xenon stripper for additional purposes. Perhaps a permanent noble-metal sink could ultimately be devised; or it is possible that a gas stripper may play some role in tritium control procedures. These potentialities may seem far fetched at this time; however, they at least remain open if the sidestream processing approach is adopted for dealing with the ^{135}Xe poisoning problem.

1.2 Disadvantages of Sidestream Processing

1.2.1 Design Uncertainty for the Stripper Unit

There is very little data available on which to base a design of a fuel salt stripper; hence, it is not possible to prove with satisfaction that any one concept is acceptable, let alone which is best. Some preliminary mass transfer data obtained for 1-in.-diam packed columns are not encouraging for considering these devices on a larger scale.

1.2.2 Larger Liquid Holdup

A key question is how small the liquid holdup can be held to in the sidestream processing unit. In this regard, iodine stripping is to be preferred over xenon stripping, and packed columns appear to be at a disadvantage.

1.2.3 Large Stripping Gas Flows Required

Whereas the gas-circulating requirement in the present MSBR reference design is a low 11 cfm, gas flows would have to be substantially higher for a sidestream stripping unit. Gas flows as high as 5600 cfm are being considered.

1.2.4 Development Work

Engineering development of the stripper and deoxidizer contactors as well as studies on fission product distribution in the gas system would likely be required. Tests on the corrosion rate in the stripper, where the fuel is made more oxidizing than in other parts of the primary system, would be needed.

2. CHEMISTRY OF IODINE STRIPPING

2.1 Laboratory Stripping Experiment

Laboratory-scale experiments were performed[1,2,3] on the removal of iodide as HI from molten LiF-BeF_2 mixtures by sparging with HF-H_2 gas mixtures, according to the reaction

$$HF(g) + I^- \rightleftharpoons F^- + HI(g) \ . \qquad (2)$$

In a typical run approximately 275 g of a molten $LiF\text{-}BeF_2$ mixture (33 to 50 mole % BeF_2) was prepared in a 2-in.-diam nickel reaction vessel as shown in Fig. 2. A weighed pellet of KI was added sufficient to bring the initial iodide concentration in the melt to approximately 1.6×10^{-5} g-mole/cm^3. The system was flushed with helium, which caused the evolution of small amounts of iodine presumably because traces of oxygen and water were initially present. Initiation of hydrogen sparging caused this evolution to cease after a short time. The HF flow was then begun at a constant partial pressure in the range 0.01 to 0.2 atm.

Hydrogen was chosen as the carrier gas to inhibit the reaction of HI(g) and nickel. Thermochemical data indicated that HI will not react with nickel to form NiI_2 and H_2 in the presence of approximately 1 atm of H_2 in the temperature range 470 to 640°C as shown in Table 1. However, as the gases are cooled to lower temperatures in the off-gas line, reaction should occur. Consequently, the off-gas line was provided with a gold liner sealed at the end to a Teflon tube. Tests in which ^{131}I tracer was used indicated that with this arrangement there was no significant holdup by adsorption of HI on the walls of the off-gas system.

Another reason for using hydrogen as a carrier gas was to inhibit the reactions by which gaseous HI dissociates,

$$HI(g) \rightleftharpoons 1/2\ I_2(g) + 1/2\ H_2(g) \ , \qquad (4)$$

$$HI(g) \rightleftharpoons I(g) + 1/2\ H_2(g) \ . \qquad (5)$$

Equilibrium constants for Eqs. (4) and (5) may be obtained from the data in Table 1, reaction (2) and (3).

---

*The equilibrium constants designated as K_i refer dissolved species to the standard state of the pure liquid and gas species to the pure gas at 1 atm. Hence, for ideal solutions, concentrations are given as mole fraction for dissolved materials and atmospheres for gases. The numerical subscript refers to reaction number given in Table 1. Equilibrium constants written as K_i' give dissolved concentrations as g-mole/cc.

ORNL-DWG-65-12055

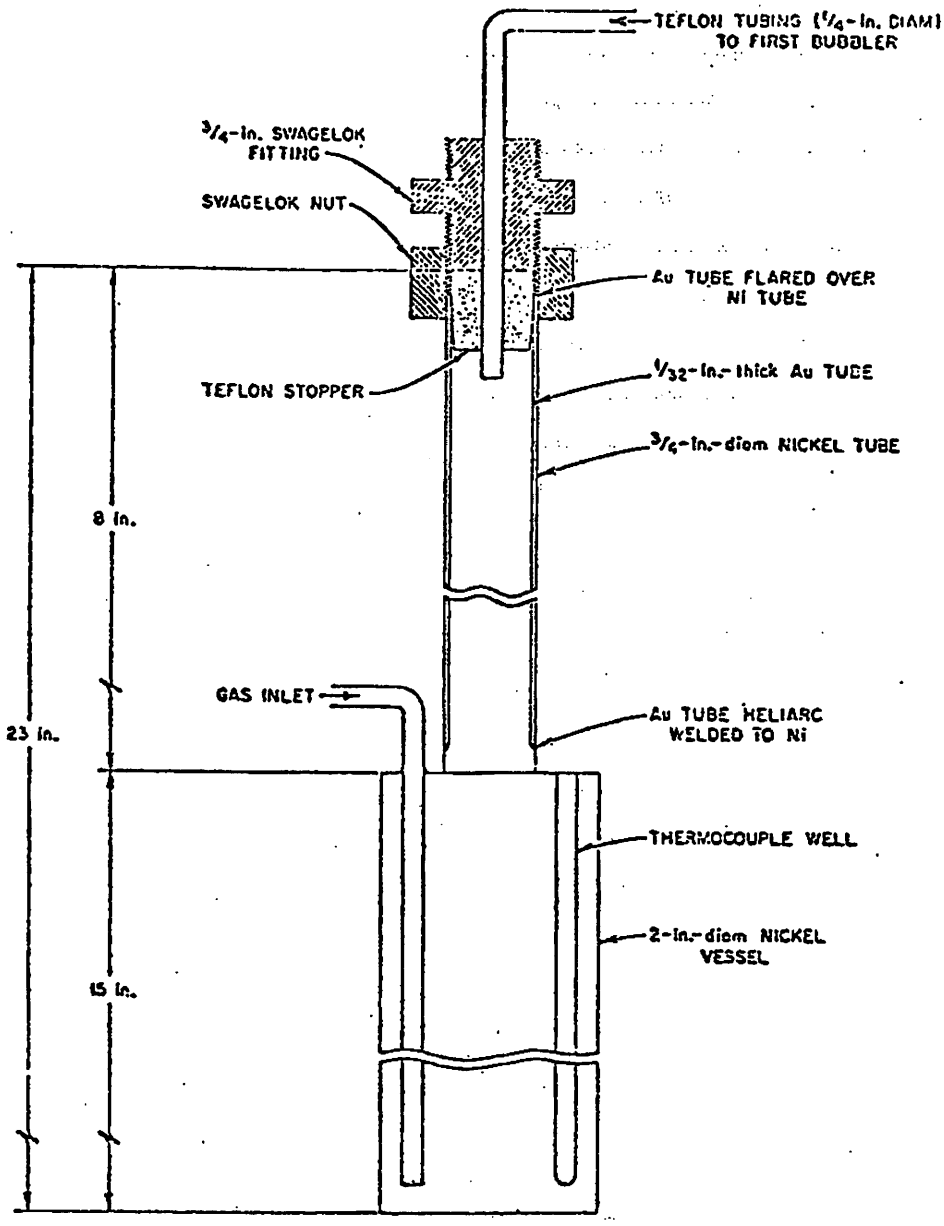

Fig. 2. Reaction Vessel Used for Iodide Removal

the conditions employed in the various runs, no more than 1% of the HI in the gas phase should dissociate, producing principally I atoms. The advantage gained by inhibiting the dissociation of HI is the simplification of the iodine chemistry in the off-gas system.

The effluent gas stream, consisting of HF, HI, and H_2, was conducted through a sintered Teflon or gold filter and subsequently to an NaOH bubbler to trap the HI. The bubbler contained a known amount of NaOH to neutralize the HI and HF, a known amount of arsenite to reduce any I_2 present, and a pH indicator. When the indicator showed that all the NaOH had been neutralized, the solution was replaced by a fresh one. In each run a series of neutralized scrub solutions was obtained, which were analyzed for iodide by potentiometric titration with standard $AgNO_3$ solution, and for I_2 by back titration of the arsenite with standard iodine solution. From the results the moles of HF, Hi, and I_2, which had entered a scrub solution, could be determined. Typically, about 95% of the iodine charged could be accounted for at the end of a run. No significant amounts of I_2 were found.

In preliminary runs, poor recoveries of iodide (typically 80%) were obtained. The cause of this was traced to small particles of salt entrained in the gaseous mixtures of HF, HI, and H_2 emerging from the reaction vessel. Evidently these particles caused condensation of HF and HI with water vapor in the NaOH bubbler. The condensed droplets of solution, readily visible as a fog in the gas phase of the trap and found to be acidic, evidently did not react completely with the NaOH solution, thus causing the low recoveries. Introduction of the filter in the off-gas line ahead of the bubbler overcame this difficulty.

Data for a typical run are plotted in Fig. 3 where it may be seen that characteristically the logarithm of the iodide concentration in the melt diminished linearly with time or with moles of HF passed. Typically, about 97 to 98% of the initial iodine charge was stripped from the melt.

Analysis of the stripping data was performed on the basis of the reaction

$$HF(g) + I^-(d) \rightarrow F^-(d) + HI(g) , \qquad (3)$$

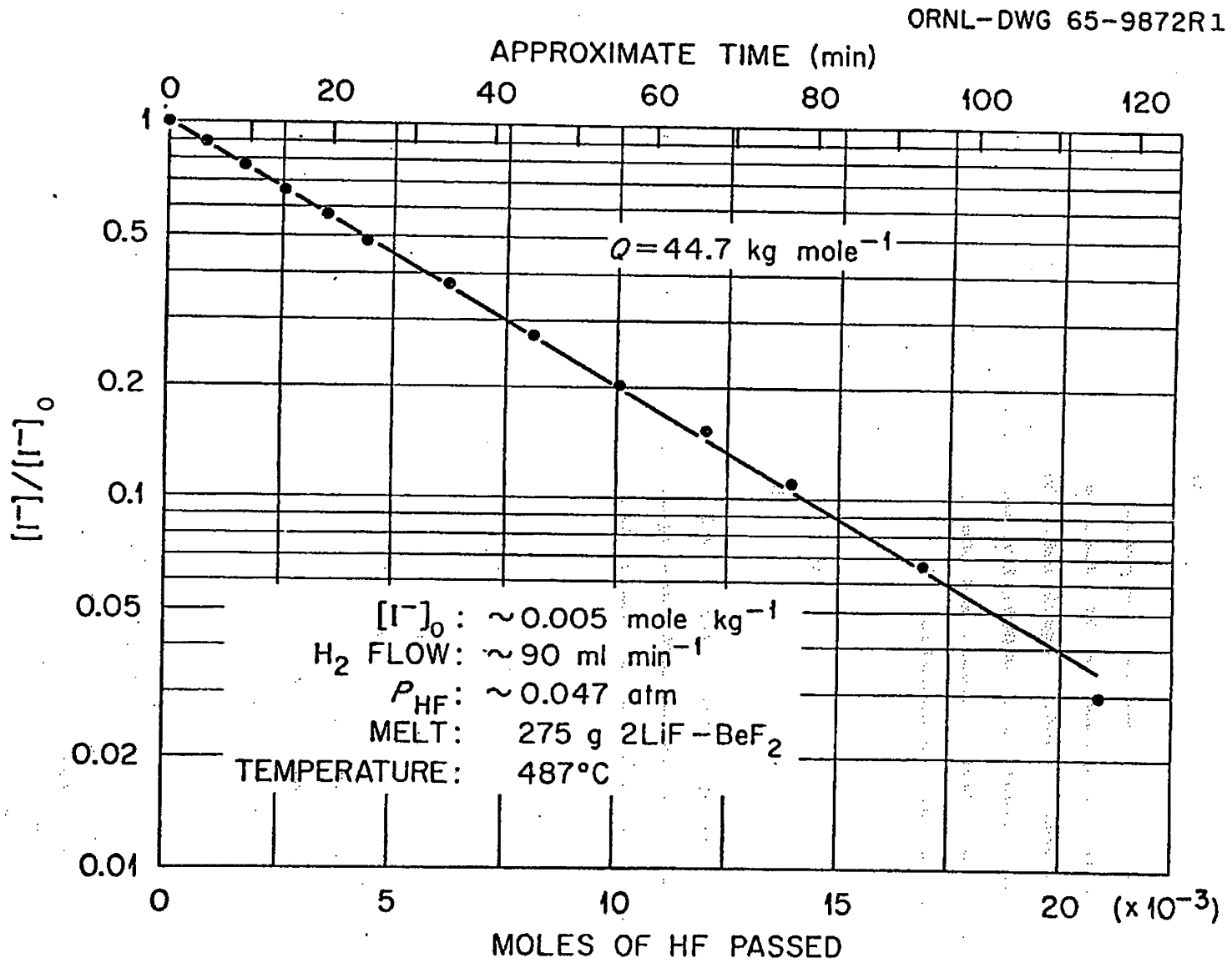

Fig. 3. Iodide Removal from L_2B as a Function of Time or Moles of HF Passed.

for which the equilibrium constant is defined as follows:*

$$K_I = \frac{P_{HI}(F^-)}{P_{HF}(I^-)} . \qquad (6)$$

Here, at the low partial pressures and the elevated temperatures involved, HF and HI are assumed to be ideal gases and hence their pressures may be used instead of their fugacities. Since, in a given experiment (i.e., for a given solvent salt composition and temperature), the activity (F^-) should have been constant and the activity (I^-) should have been proportional to the concentration $[I^-]$, it is convenient to define

$$K_I' = \frac{P_{HI}}{P_{HF}[I^-]} , \qquad (7)$$

which, like K_I, should vary solely with temperature.

If it is now assumed that equilibrium was continuously maintained between the salt and gas phase, then there results[1]

$$\ell n \frac{[I^-]}{[I^-]_o} = -\frac{K_I'}{V} n_{HF} , \qquad (8)$$

where $[I^-]_o$ is the initial iodide concentration, V the volume of the melt, and n_{HF} the moles of HF passed. Thus, the value of K_I' presumably may be determined from the slope of $\ell n\ [I^-]/[I^-]_o$ vs n_{HF} or time, since the sparge flow was constant. Though this assumption corroborates the observed linear decrease of $\ell n\ [I^-]$ with n_{HF} shown in Fig. 3**, it was

---

*The designation (F^-) signifies activity of F^-, $[F^-]$ concentration in g-moles/cc and X_{F^-} mole fraction.

**The data points in Fig. 3 are actually data corrected to account for small unavoidable losses of iodine ($n_{I,\ell}$) incurred prior to starting the run. Values of $n_{I,\ell}$ and K_I' were computed to yield the least squares line shown in Fig. 3.

nevertheless ultimately determined that assuming equilibrium between the gas and liquid phases was not correct. Equation (8) should properly be written,

$$\ell n \frac{[I^-]}{[I^-]_o} = - \frac{K_{app}}{V} n_{HF} , \qquad (8a)$$

where K_{app} is written in place of K to indicate that the value of the equilibrium constant computed by means of Eq. (8) is wrong. This was first noted when it became clear that computed values of the equilibrium constant were dependent on the partial pressure of HF in the fashion shown in Fig. 4. The reciprocal of the equilibrium constant is seen to increase linearly with P_{HF} for each of the three melt compositions tested – which, of course, would not be the case if all the assumptions made were valid.

A number of reasons for the variation of K_{app} with P_{HF} were proposed:[3]

1. The possibility of a chemical reaction competing with Eq. (3) could not be ruled out.

2. Baes[4] showed that if HI(d) exists uniformly distributed throughout the melt, the instantaneous equilibrium exists between the melt and sparge gas, then $1/K$ will vary linearly with P_{HF} with the slope of the line equal to K_{HI}, the solubility coefficient for HI. The difficulty, however, arose when it was observed that K_{HI} had to be quite high to yield the observed variation.

3. The third posulated explanation is that equilibrium conditions were not established between the melt and the sparge gas. As the partial pressure of HF was increased, so too was the departure from equilibrium.

The model proposed in the next section has evidently resolved this question satisfactorily. It is shown that if one assumes the stripping rate to be limited by the diffusion of I^- to the surface, the variation observed in Fig. 4 results. Hence, the following proposed mechanism is essentially a quantified version of postulate (3) above.

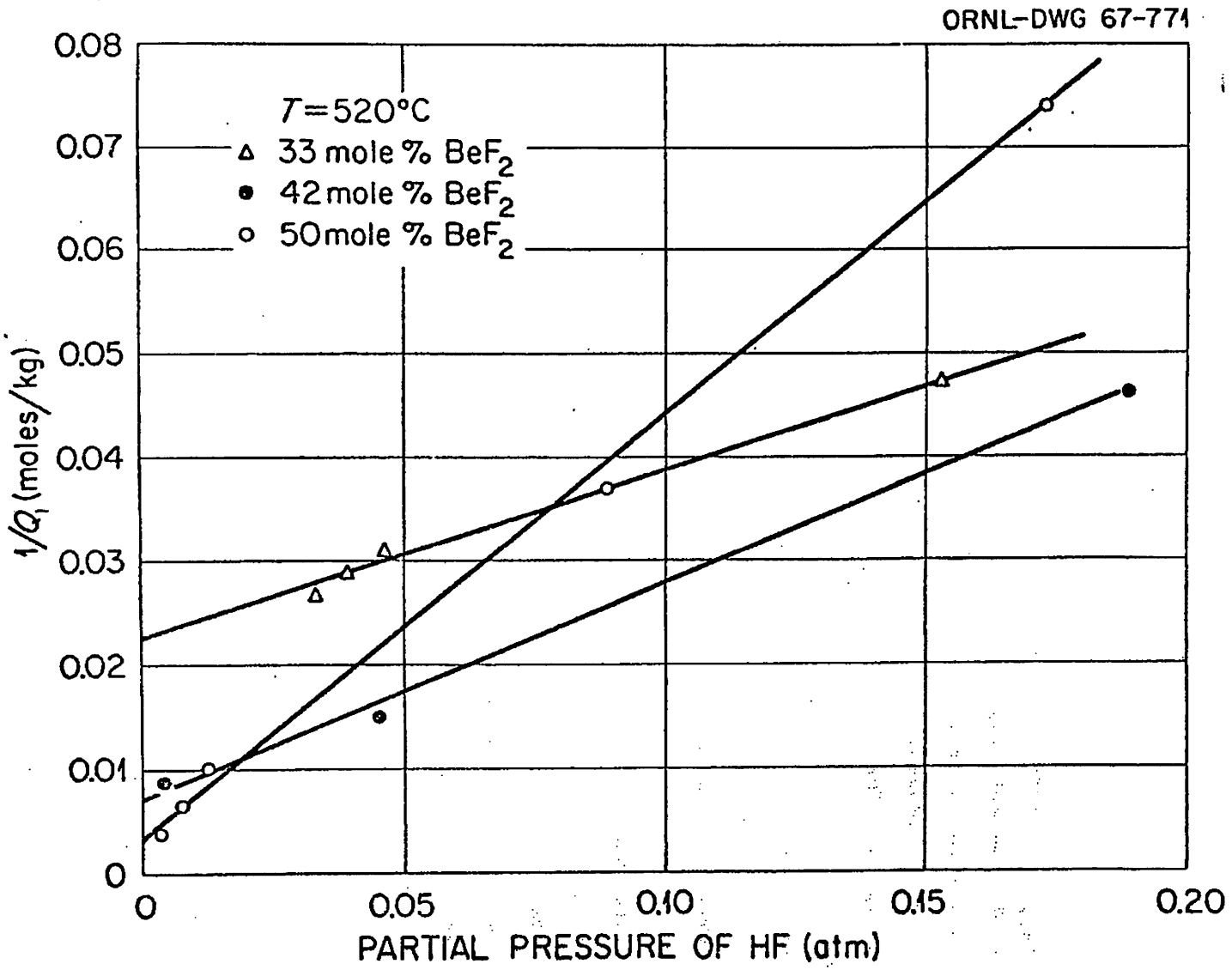

Fig. 4. Variation of Q_1 (Related to Apparent Equilibrium Constant) with P_{HF}.

2.2 Analysis of the Iodine Desorption Mechanism

2.2.1 Description of Model

Several chemical models for the desorption process in this experiment were considered. The following one was found to be in agreement with the two distinctive features of the sparging data, namely, the linear decay of the logarithm of the iodine content of the salt with moles of HF passed (Fig. 3) and the linear increase of the reciprocal of the equilibrium quotient with the partial pressure of HF in the sparge gas (Fig. 4).

Referring to Fig. 5, the proposed model assumes the rate-controlling step to be the transport of I^- from the bulk liquid to a surface reaction zone. In comparison, the transport rate of HF(g) to the liquid surface, the adsorption rate of HF, and the liquid phase reaction

$$H^+ + I^- \rightarrow HI(d) \tag{9}$$

are assumed to be rapid. Additionally, the desorption and removal rates of HI are assumed to be rapid. The above reaction is assumed to take place in a narrow region near the surface, throughout which concentrations are uniform and governed by the equilibrium relation,

$$K' = \frac{[HI]^*}{[H^+]^*[I^-]^*}, \tag{10}$$

where the asterisk signifies that the variable pertains to the surface zone. The proton concentration, $[H^+]^*$, is governed by the partial pressure of HF in the sparge gas and the solubility coefficient for HF,

$$[H^+]^* = K_{HF} P_{HF} . \tag{11}$$

The sparging rate and the HF partial pressure in the feed gas remained constant throughout each run. Since typically about 10,000 times the required stoichiometric amount of HF was passed, it may be safely assumed that the surface proton concentration was constant throughout the vessel and during the runs.

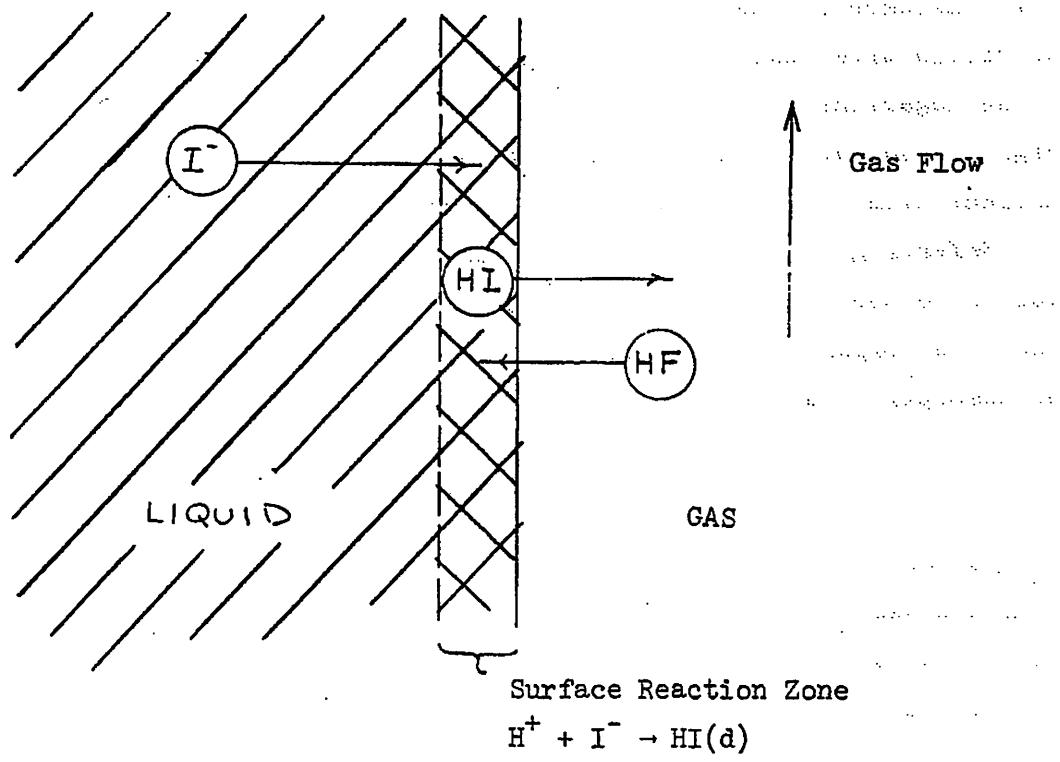

Fig. 5. Model for Desorption of Iodide from Lithium-Beryllium Fluoride by Sparging with HF.

If the volume of the surface zone is small compared with the bulk liquid, and if no molecular HI exists in the bulk liquid, the following balance holds,

$$V \frac{d[I^-]}{dt} = - h_m A_b \left([I^-] - [I^-]^* \right), \qquad (12)$$

where h_m is the mass transfer coefficient to the bubble surfaces of total area A_b. Similarly, the mass transfer rate of I^- to the liquid surface must equal the iodine removal rate as HI in the sparge gas, i.e.,

$$h_m A_b \left([I^-] - [I^-]^* \right) = [HI]_g Q_g . \qquad (13)$$

The concentration, $[HI]_g$, is related to the liquid surface concentration of HI via the solubility coefficient, K_{HI}, and the ideal gas law,

$$[HI]^* = K_{HI} [HI]_g RT . \qquad (14)$$

Thus, Eq. (13) may be written,

$$h_m A_b \left([I^-] - [I^-]^* \right) = \frac{[HI]^* Q_g}{K_{HI} RT} . \qquad (15)$$

Equations (10), (12), and (15) may be solved simultaneously for the unknown functions of time, $[I^-]$, $[I^-]^*$, $[HI]^*$. Substituting Eqs. (10) and (15) into (12) yields,

$$V \frac{d[I^-]}{dt} = - \left(\frac{\left(h_m A_b [H^+]^* \right) Q_g}{h_m A_b \frac{K_{HI}}{K'} RT + [H^+]^* Q_g} \right) [I^-] . \qquad (16)$$

Hence the iodine concentration as a function of time in the batch stripper is given by

$$[I^-] = [I^-]_o e^{-Ct} , \qquad (17)$$

where

$$C \equiv \frac{h_m A_b [H^+]^* Q_g}{h_m A_b \frac{K_{HI}}{K'} RTV + [H^+] Q_g V} \cdot = \frac{1}{\text{sec}} \qquad (18)$$

Note that the independent variable is time, and that n_{HF}, the moles of HF passed, is of significance only if it relates to the time required. The two variables are directly related by,

$$n_{HF} = \left(\frac{P_{HF} Q_g}{RT} \right) t \cdot \qquad (19)$$

Equations (17) and (19) are consistent with the observed linear decrease of $\ell n[I^-]$ with n_{HF} shown in Fig. 3 for a typical run. Note also that in no way may the values at K' and K_{HI} be separately determined. The ratio K'/K_{HI} may, however, be evaluated from a single batch sparging run from Eqs. (17) and (18) provided the mass transfer coefficient, h_m, and bubble surface area, A_b, are known. However, a superior way to evaluate this parameter is given below.

2.2.2 Evaluation of K'/K_{HI}

An accurate determination of the quotient K'/K_{HI} may be obtained from a series of batch sparging experiments at various HF partial pressures from which the mass transfer effect may be eliminated by extrapolation to zero HF pressure. For this purpose define a slope, m, of $\ell n[I^-]$ relative to the number of moles of HF passed,

$$m \equiv - \frac{d\, \ell n \left([I^-]/[I^-]_o \right)}{d\, n_{HF}} \cdot \qquad (20)$$

This slope may be related to the constant, C, which is the slope of $\ell n[I^-]$ vs time, by using Eq. (19); thus,

$$m = \frac{CRT}{P_{HF} Q_g} \cdot \qquad (21)$$

Substituting the expression for C from Eq. (18) into Eq. (21) yields,

$$\frac{1}{m} = \frac{K_{HI}}{K'} \frac{V}{K_{HF}} + \frac{Q_g V}{h_m A_b RT} P_{HF} . \qquad (22)$$

The reciprocal of the slope, m, plotted vs P_{HF} should be linear with intercept $(K_{HI}/K')(V/K_{HF})$. Similarly, the rate of increase of 1/m with P_{HF} is seen to be related to the mass transfer product, $h_m A_b$, in the salt, the rate of increase being steepest when the mass transfer rate is small.

It may be noted that m is directly related to the apparent equilibrium quotient, K'_{app}, defined for Eq. (3). Comparison of Eqs. (20) and (8a) indicates that

$$K'_{app} = - mV . \qquad (23)$$

To match the units used for Fig. 4, define

$$Q_1 \equiv K'_{app} \cdot \rho = - mw \qquad (24)$$

where ρ is the melt density in kg cc and w is the mass of the melt in kilograms. Substitution of Eq. (24) into (22) yields,

$$\frac{1}{Q_1} = \frac{K_{HI}}{K'} \frac{V}{K_{HF} w} + \frac{QV}{h_m A_b RT w} P_{HF} . \qquad (25)$$

Referring to Fig. 4, we see that in fact the data have shown the linear relationship between $1/Q_1$ and P_{HF} predicted by Eq. (25). The intercept for the 33 mole-% BeF_2 line is seen to be 0.022 g-mole/kg, from which it is found that

$$\frac{K_{HI}}{K'} = 7.8 \times 10^{-10} \left(\frac{\text{g-mole}}{\text{cc}}\right) \frac{1}{\text{atm}} ,$$

taking w/V to be 0.0020 kg/cc and K_{HF} equal to 17.8×10^{-6} g/cc-atm appropriate for HF over L_2BF_4 at 520°C.

Note that K_{11} for reaction (11) given in Table 1 is equivalent to K_{HI}/K' allowing for the different units. From the values of the constants a and b given in Table 1, the value

$$K'_{11} = 5.95 \times 10^{-10} \left(\frac{\text{g-mole}}{\text{cc}}\right)^2 \frac{1}{\text{atm}}$$

is obtained at t = 520°C, the temperature of the laboratory experiments. The value of K_{11} obtained from Table 1 will be employed for the stripping calculations in the following sections rather than the intercept value for K_{HI}/K' primarily to obtain a proper temperature variability for the iodine desorption reactions.

2.2.3 Comparison of $h_m A_b$ with Empirical Correlations

In this section we seek to verify that the observed mass transfer rates, as determined from the slope of $1/Q_1$ vs P_{HF}, are in fact within the range that may be anticipated in this sort of an experiment.

From Fig. 4 for L_2BF_4 salt and Eq. (25) determine from the slope,

$$\frac{Q_g V}{h_m A_b RTW} = 0.16 \frac{\text{g-mole}}{\text{kg-atm}} .$$

The average value of the sparge gas flow was 3.12 cm^3/sec, and taking the salt density to be 0.002 kg/cm^3 yields,

$$h_m A_b = 0.15 \text{ cm}^3/\text{sec} .$$

In sparging experiments, experience has shown that bubble diameters invariably range between 1/8 and 1/4 in.[5] Assuming an average diameter of 3/16 in. indicates that approximately 55 bubbles/sec were produced in the experiment. The terminal rise velocity for a bubble of this size is estimated to be 29 cm/sec from the empirical equation applicable in the intermediate range of bubble Reynolds numbers. Hence, each bubble resides in the sparge vessel approximately 0.3 sec since the liquid height was ~8.6 cm, for total number of bubbles in residence of 55 × 0.3 = 17. Thus, A_b is determined to be approximately 12 cm^2, which results in a value for h_m of 0.013 cm/sec (1.5 ft/hr).

An empirical equation for h_m for the case of swarming bubbles is given by Schaftlein and Russel[6] to be,

$$Sh = 2.0 + 0.0187 \left[Re_b^{0.484} Sc^{0.339} \left(\frac{d_b \, g^{1/3}}{D^{2/3}} \right)^{0.072} \right]^{1.61} \quad . \qquad (26)$$

For the present case, $Re_b = 208$ and $d_b = 0.48$ cm. Additionally, assuming $Sc = 1700$ and the diffusivity, D, to be 1.3×10^{-5} cm^2/sec, yields $Sh = 520$, and thus, $h_m = 0.014$ cm/sec.

The very close comparison between h_m determined from the slope of $1/Q_1$ vs P_{HF} and that estimated from Eq. (26) is, of course, coincidental. It is only significant that the two values are not inconsistent, and hence the observed rate of variation of the equilibrium quotient, Q_1, with HF partial pressure may indeed be reasonably accounted for by the proposed mechanism.

Further, we may note that trend of the slope in Fig. 4 with BeF_2 content in the melt is in the proper direction. Since the slope should vary inversely with the mass transfer coefficient in accord with Eq. (26), increasing the BeF_2 concentration with the attendant rise in viscosity of the melt should cause the increase in slope observed in Fig. 4.

Summarizing then, we may express some confidence that the mechanism for desorption of iodine from LiF-BeF_2 melts is well understood. The observed linear decrease of $[I^-]$ in the melt with time is in accord with the postulated model, as also is the variation of $1/K'_{app}$ with P_{HF} in the sparge gas. The value of the slope is consistent with estimated values of the mass transfer coefficient obtained from empirical formula for sparging contactors. Finally, the trend of the slope with BeF_2 content in the melt is consistent with the viscosity variation with increasing BeF_2 concentrations.

2.3 Chemistry of Iodine Desorption in MSBR Fuel

In this section some of the significant differences between the chemical environment of laboratory experiments and that to be encountered

in the primary loop of a reactor will be discussed. While the iodine stripping reaction from lithium-beryllium fluoride melts appears to be well understood, stripping from fuel salt presents numerous additional problems. Frequent reference will be made to the reactions and equilibrium constants listed in Table 1, which though pertaining specifically to reactions involving L_2BF_4 melts are not expected to be greatly different for MSBR fuels.

2.3.1 Maximum Allowable U^{+4}/U^{+3} Ratio

The behavior of iodine in an MSBR, as will be seen, should be strongly dependent on the state of oxidation of the fuel. This will be reflected in the ratio $[U^{4+}]/[U^{3+}]$. The upper and lower limits of this ratio in the fuel circuit should be set by the following considerations: (1) The concentration of Ni^{2+} in the fuel, produced by the reaction

$$2U^{4+} + Ni^0 \rightleftharpoons Ni^{2+} + 2U^{3+} \qquad (27)$$

probably should not exceed 0.1 ppm, to keep the mass transfer of nickel at acceptably low levels. (2) The ratio $[U^{3+}]/[Pa^{4+}]$ should not fall below the limit set by the equilibrium

$$5/4UO_2(c) + Pa^{4+} \rightleftharpoons U^{3+} + 1/4U^{4+} + 1/2Pa_2O_5(c) \qquad (28)$$

otherwise Pa_2O_5 could precipitate at an even lower level of oxide contamination than would UO_2. (3) The ratio $[U^{4+}]/[U^{3+}]$ should not fall below the value corresponding to the equilibrium

$$U^{3+} + \frac{X}{4} C^0 \rightleftharpoons 3/4U^{4+} + 1/4UC_X(c) , \qquad (29)$$

which results in the formation of a uranium carbide. Assuming that $X_{U^4} = 0.003$ and $X_{Pa^{4+}} = 1.4 \times 10^{-5}$ (100 ppm) the equilibrium constants for these reactions (18, 21, and 22 in Table 1) yield the following limits for the $[U^{4+}]/[U^{3+}]$ ratio over this temperature range expected in an MSBR:

Table 1. Equilibria Related to the Behavior of Iodine in LiF-BeF_2 (67-33 mole %)
log K = a + b (10^3/T), (700 to 1000°K)

Reaction	K	a	b	$\sigma_{\log K}$	log K(600°)	Source[a]
(1) $HF(g) + I^- = F^- + HI(g)$	$(P_{HI})/(P_{HF})(X_{I^-})$	0.06	2.42	0.08	2.83	Fig. 4
(2) $HI(g) = I(g) + \frac{1}{2}H_2(g)$	$(P_I)(P_{H_2})^{\frac{1}{2}}/(P_{HI})$	2.35	- 4.35	0.02	- 2.63	JANAF
(3) $I(g) = \frac{1}{2}I_2(g)$	$(P_{I_2})^{\frac{1}{2}}/(P_I)$	-2.74	4.00			JANAF
(4) $HF(g) + I^- = I(g) + \frac{1}{2}H_2(g)$	$(P_{H_2})^{\frac{1}{2}}(P_I)/(P_{HF})(X_{I^-})$	2.41	- 1.93	0.08	0.20	(1) + (3)
(5) $\frac{1}{2}H_2(g) + U^{4+} + F^- = U^{3+} + HF(g)$	$(P_{HF})(X_{U^{3+}})/(P_{H_2})^{\frac{1}{2}}(X_{U^{4+}})$	4.07	- 9.33	0.02	- 6.62	LB
(6) $I^- + \frac{1}{2}H_2(g) + U^{4+} = U^{3+} + HI(g)$	$(P_{HI})(X_{U^{3+}})/(P_{H_2})^{\frac{1}{2}}(X_{I^-})(X_{U^{4+}})$	4.13	- 6.91	0.08	- 3.78	(1) + (5)
(7) $I^- + U^{4+} = U^{3+} + I(g)$	$(P_I)(X_{U^{3+}})/(X_{I^-})(X_{U^{4+}})$	6.48	-11.26	0.09	- 6.42	(1) + (3) + (5)
(8) $I(g) = I(d)$	$(X_I)/(P_I)$	-4.25	- 2.75		- 7.40	EST
(9) $I^- + U^{4+} = U^{3+} + I(d)$	$(X_I)(X_{U^{3+}})/(X_{I^-})(X_{U^{4+}})$	2.23	-14.01		-13.82	(1) + (3) + (5) + (8)
(10) $HF(g) = H^+ + F^-$	$(X_{H^+})/(P_{HF})$	-5.17	1.31	0.02	- 3.67	FS
(11) $HI(g) = H^+ + I^-$	$(X_{H^+})(X_{I^-})/(P_{HI})$	-5.23	- 1.11	0.08	- 6.50	-(1) + (10)
(12) $H_2(g) = H_2(d)$	$(X_{H_2})/(P_{H_2})$	-4.42	- 1.55	0.5	- 6.20	M
(13) $\frac{1}{2}H_2(d) + U^{4+} = U^{3+} + H^+$	$(X_{H^+})(X_{U^{3+}})/(X_{H_2})^{\frac{1}{2}}(X_{U^{4+}})$	1.11	- 7.25	0.3	- 7.19	(5) + (10) - $\frac{1}{2}$(12)
(14) $2HF(g) + Ni^0 = Ni^{2+} + 2F^- + H_2(g)$	$(P_{H_2})(X_{Ni^{2+}})/(P_{HF})^2$	-8.37	3.60	0.04	- 4.25	B
(15) $2HF(g) + Ni^0 = NiF_2(c) + H_2(g)$	$(P_{H_2})/P_{HF}^2$	-8.67	5.67	0.04	- 2.18	B
(16) $2HI(g) + Ni^0 = Ni^{2+} + 2I^- + H_2(g)$	$(P_{H_2})(X_{Ni^{2+}})(X_{I^-})^2/(P_{HI})^2$	-8.49	- 1.24	0.16	- 9.91	-2(1) + (14)
(17) $2HI(g) + Ni^0 = NiI_2(c) + H_2(g)$	$(P_{H_2})/(P_{HI})^2$	-8.4	+ 4.3	0.7	- 3.5	KB
(18) $Ni^0 + 2U^{4+} = 2U^{3+} + Ni^{2+}$	$(X_{Ni^{2+}})(X_{U^{3+}})^2/(X_{U^{4+}})^2$	-0.24	-15.06	0.06	-17.48	2(5) + (14)
(19) $\frac{5}{4}UO_2(c) + Pa^{5+} = \frac{5}{4}U^{4+} + \frac{1}{2}Pa_2O_5(c)$	$(X_{U^{4+}})^{\frac{5}{4}}/(X_{Pa^{5+}})$	-5.94	+ 7.01	0.12	2.09	RBB
(20) $Pa^{4+} + U^{4+} = Pa^{5+} + U^{3+}$	$(X_{Pa^{5+}})(X_{U^{3+}})/(X_{Pa^{4+}})(X_{U^{4+}})$	5.81	- 9.82	0.5	- 5.44	RBB
(21) $\frac{5}{4}UO_2(c) + Pa^{4+} = \frac{1}{4}U^{4+} + U^{3+} + \frac{1}{2}Pa_2O_5(c)$	$(X_{U^{4+}})^{\frac{1}{4}}(X_{U^{3+}})/(X_{Pa^{4+}})$	-0.13	- 2.81	0.5	- 3.35	(19) + (20)
(22) $U^{3+} + \frac{x}{2}C^0 = \frac{3}{4}U^{4+} + \frac{1}{4}UC_x(c)$	$(X_{U^{4+}})^{\frac{3}{4}}/(X_{U^{3+}})$	-4.16	6.05		2.77	T
(23) $H^+ + U^{+3} = U^{+4} + \frac{1}{2}H_2(g)$	$(X_{U^{4+}})(P_{H_2})^{\frac{1}{2}}/(X_{U^{3+}})(X_{H^+})$	1.11	9.02			$-\frac{1}{2}$(12) - (13)

[a] JANAF: Values derived from JANAF Thermochemical Tables, 2nd ed., 1971.
LB: G. Long and F. F. Blankenship, ORNL-TM-2065 II, November 1969.
EST: Estimated assuming that the solubility of I is similar to that of Xe, measured by G. M. Watson, R. B. Evans III, W. R. Grimes, and N. V. Smith, J. Chem. Eng. Data, 7(2): 285 (1962).
FS: P. E. Field and J. H. Shaffer, J. Phys. Chem., 71: 3218 (1967).
M: Estimated by A. P. Malinauskas, as reported in MSR Program Monthly Report, September 1970, MSR-70-79.
B: C. M. Blood, ORNL-CF-61-5-4, September 1961.
KB: Calculated from ΔH^f [$NiF_2(c)$] = 23 ± 2 kcal (O. Kubaschewski, E. L. Evans, and C. B. Alcock, Metallurgical Thermochemestry, 4th ed., Pergamon Press, 1967), ΔS = 35 e.u. (L. Brewer, in "The Chemistry and Metallurgy of Miscellaneous Materials: Thermodynamics", L. L. Quill (ed.), pp. 76-192, McGraw-Hill, New York (1950).
RBB: R. G. Ross, C. E. Bamberger, and C. F. Baes, Jr.,
T: L. M. Toth, p. 9, Reactor Chem. Div. Ann. Progr. Rept. May 31, 1971, ORNL-4717.

	$[U^{4+}]/[U^{3+}]$	
Condition	550°C	700°C
$X_{Ni^{2+}}$ <0.1 ppm	$<10^{5.6}$	$<10^{4.2}$
Pa_2O_5 more soluble than UO_2	$<10^{5.2}$	$<10^{4.7}$
U^{3+} does not react with graphite	$>10^{2.5}$	$>10^{1.4}$

Thus it may be concluded that the $[U^{4+}]/[U^{3+}]$ ratio should be held within the approximate limits of $10^{2.5}$ to $10^{4.2}$. Since iodine stripping is enhanced in an oxidizing environment, it will be assumed here that the U^{+4}/U^{+3} ratio in the primary loop is set at 10^4, very near the allowable upper limit.

2.3.2 Iodine Species in Liquid and Gas Phases

From reaction [9], Table 1, we may determine that at 700°C,

$$\frac{[I](d)}{[I^-](d)} = 10^{-12.2}\ U\ ,$$

where the symbol U is used for U^{+4}/U^{+3} for brevity. Since the maximum value for U has been established as approximately 10^4 for the MSBR primary system, the ratio of atomic iodine to iodide is thus $\sim 10^{-8}$ for fuel salt at 700°C. At lower temperatures, the ratio is lower still. Molecular iodine will likely be present in still smaller amounts due to the extremely small concentration of iodine in the fuel, making association to I_2 an extremely unlikely event. Thus, we conclude that the only significant species of iodine in the fuel will be iodide ion — as was the case for stripping experiments using LiF + BeF_2 melts.

On the other hand, the off-gas composition will be quite different since the carrier gas will undoubtedly be helium rather than hydrogen. Thus the fraction of iodine as HI will be smaller with proportionately larger amounts of I(g). From the definition of the equilibrium constants K_2 and K_3, it may readily be shown that the concentration of atomic iodine in the stripping gas is given by,

$$[I](g) = \frac{-\left(\sqrt{\frac{P_{H_2}}{K_2}} + 1\right) + \sqrt{\left(\sqrt{\frac{P_{H_2}}{K_2}} + 1\right)^2 + 8K_3^2\, RT\, (P/Q_g)}}{4\, K_3^2\, RT} \qquad (30)$$

where P and Q_g, respectively, are the production rate of iodine and the stripping gas volumetric flowrate. Steady state is presumed for Eq. (30) to apply, in which case the ratio P/Q_g represents the total g-moles of iodine per unit volume of stripping gas for those isotopes that decay slowly with respect to removal time. Thus Eq. (30) would apply to ^{135}I for removal times substantially less than 6.7 hr.

Substitution of typical values into Eq. (30) shows that the second term in the square root is small compared with the first which allows the following simplification:

$$\text{Fraction of iodine as } I(g) = \frac{1}{\left(1 + \sqrt{\frac{P_{H_2}}{K_2}}\right)}, \qquad (31)$$

$$\text{Fraction of iodine as } HI(g) = \frac{\sqrt{P_{H_2}}}{K_2\left(1 + \sqrt{\frac{P_{H_2}}{K_2}}\right)}. \qquad (32)$$

Equations (31) and (32) are plotted in Fig. 6 vs hydrogen partial pressure. It is seen that when P_{H_2} is less than $\sim 10^{-5}$ atmospheres, iodine exists in the purge gas primarily as I(g) when t = 1300°F. Lower temperatures favor HI relative to atomic iodine.

From the definition of K_3 we may write,

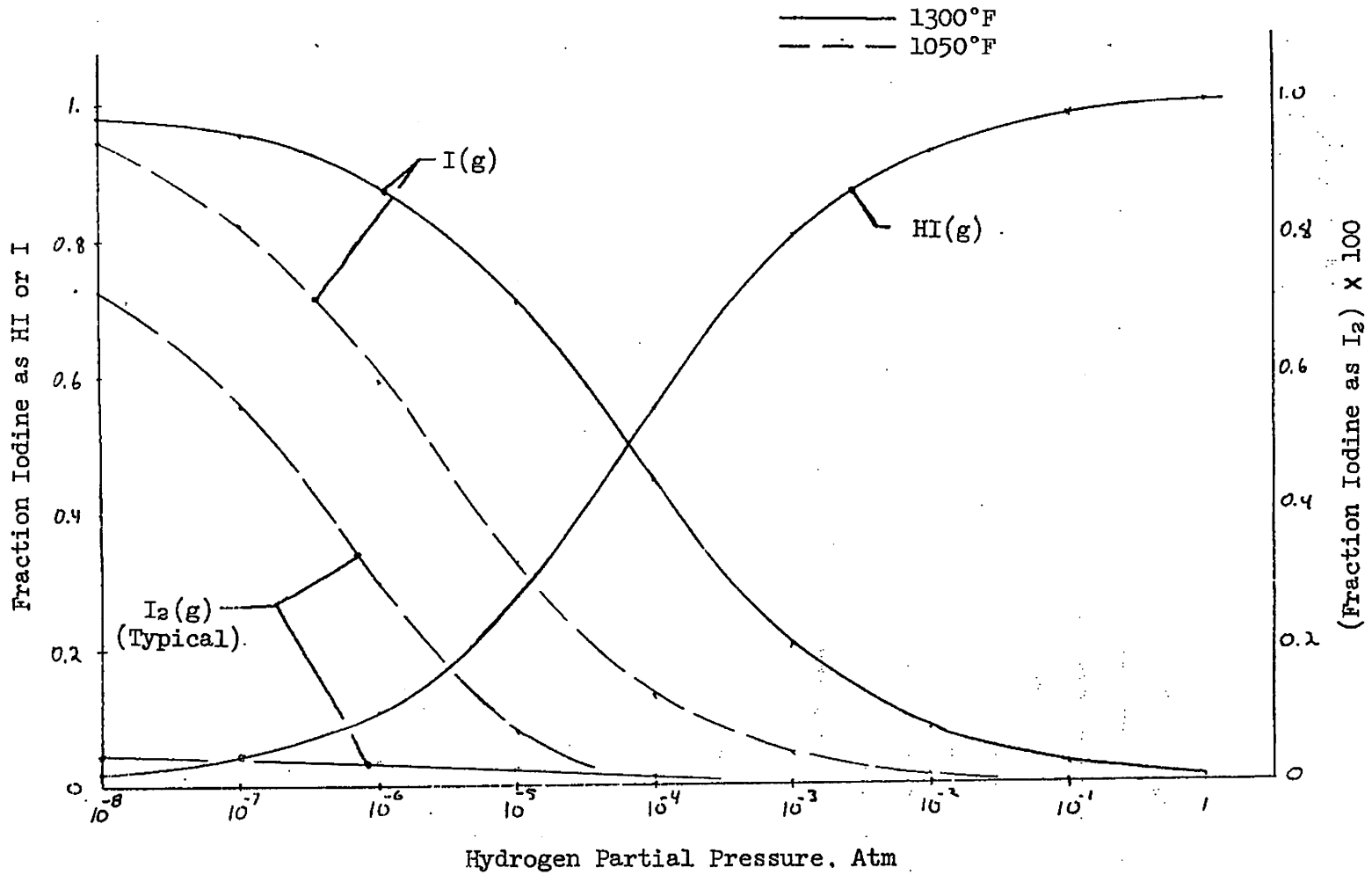

Fig. 6. Iodine Species in the Stripping Gas as a Function of Hydrogen Partial Pressure.

$$\text{Fraction of iodine as } I_2(g) = \frac{K_3^2\, RT\, (P/Q_g)}{\left(1 + \sqrt{\frac{P_{H_2}}{K_2}}\right)^2}, \qquad (33)$$

which is also plotted in Fig. 6 using a typical value of 10^{-11} (g-mole/cc) for P/Q_g. The result illustrates that while association to $I_2(g)$ is thermodynamically favored, the very low concentrations of iodine allow only small amounts of $I_2(g)$ to form. Low hydrogen pressure and low temperatures favor formation of molecular iodine.

2.3.3 Effective Solubility of Iodine in Fuel Salt

A convenient way of expressing the ease or difficulty with which iodine may be stripped from fuel is by means of the effective solubility coefficient defined by,

$$K_{eff} = \frac{[I^-]}{P_{HI} + P_I}, \ \frac{\text{g-mole}}{\text{cc-atm}}. \qquad (33)$$

Thus K_{eff} denotes the ratio of iodide ion in the melt in equilibrium with the two significant species of gaseous iodine. Contrary to the solubility coefficient for a single solute, which is a function solely of temperature, the value of K_{eff} will be determined by the chemical environment as well.

The significance of K_{eff} may be illustrated by considering a hypothetical counterflow stripping device in which the gas and liquid phases are in equilibrium at the rich end. If solute free gas is assumed to enter the lean end, then a mass balance yields the result,*

$$\frac{Q_g}{Q_\ell} = \eta\, KRT, \qquad (34)$$

*See Section 3.1.

where the left hand side represents the ratio of the volumetric flows of the gas and liquid phases to achieve a given stripping efficiency, η, for a given value of the solubility coefficient, K. Some typical values for this relative phase ratio at a 1000°K and 100% stripping efficiency are given in Table 2. Note that for xenon, equilibrium requires only minute gas flow; hence, the volumetric gas requirements for xenon strippers are determined entirely by other considerations. Even for a far more soluble material like HF, stripping gas requirements are not excessive from solely a chemical equilibrium point of view. We shall see that iodine is far more difficult to strip than HF under acceptable conditions in the stripping device.

Table 2. Some Typical Values of the Ratio Q_g/Q_ℓ

	$K\left(\frac{\text{g-mole}}{\text{cc-atm}}\right)$	Q_g/Q_ℓ for $\eta = 1$
Xenon	5×10^{-9}	4×10^{-4}
Hydrogen fluoride	5.5×10^{-6}	0.44

Thus the value of K_{eff}, together with the phase flow ratio as determined from Eq. (34), is useful for scanning the range of permissible variables for the best possible set of values. This is in no way a stripper design procedure; merely a convenient way of initially selecting some attractive operating conditions.

In the laboratory experiments, where the formation of I(g) was suppressed by the use of hydrogen carrier gas, an expression for K_{eff} may be derived by simply noting that for the reactions

$$H^+ + I^- \rightleftharpoons HI(d) \text{ , and} \tag{35a}$$

$$HI(d) \rightleftharpoons HI(g) \text{ .} \tag{35b}$$

The value for P_{HI} is given by $\frac{K'[I^-][H^+]}{K_{HI}}$. Here,

$$K_{HI} \equiv \frac{[HI](d)}{P_{HI}} \text{ , and}$$

$$K' \equiv \frac{[H^+][I^-]}{[HI](d)} .$$

Thus, Eq. (33) yields for stripping iodine from lithium-beryllium salts,

$$K_{eff} = \frac{K_{HI}}{K' [H^+]} , \tag{36}$$

where the protons are supplied by the dissolution of HF present in the stripping gas.

A primary system iodine stripper presents a more complex chemical environment than existed in the laboratory experiments. First, as already noted, both I(g) and HI(g) exist in the gas phase whereas formation of I(g) was suppressed in the laboratory. A second difference is the presence of U^{+4} in fuel salt which may oxidize iodide via

$$I^- + U^{+4} \rightleftharpoons I(d) + U^{+3} , \tag{37}$$

with I(d) subsequently desorbing,

$$I(d) \rightleftharpoons I(g) . \tag{38}$$

A third point of difference is that whereas protons for the reaction given in Eq. (35a) were supplied solely by HF in the stripping gas for the L_2B experiments, fuel salt will naturally contain some concentration of protons, depending primarily on the level of hydrogen inleakage into the primary system and the U^{+4}/U^{+3} ratio of the fuel. Figure 7 illustrates the situation for stripping iodine from fuel salt.

Thus, two expressions may be obtained for K_{eff}, one for each of the parallel paths for iodine removal: (1) reaction of iodide with H^+ and desorption of HI, and (2) oxidation by U^{+4} and desorption of I. For the first case substitution of

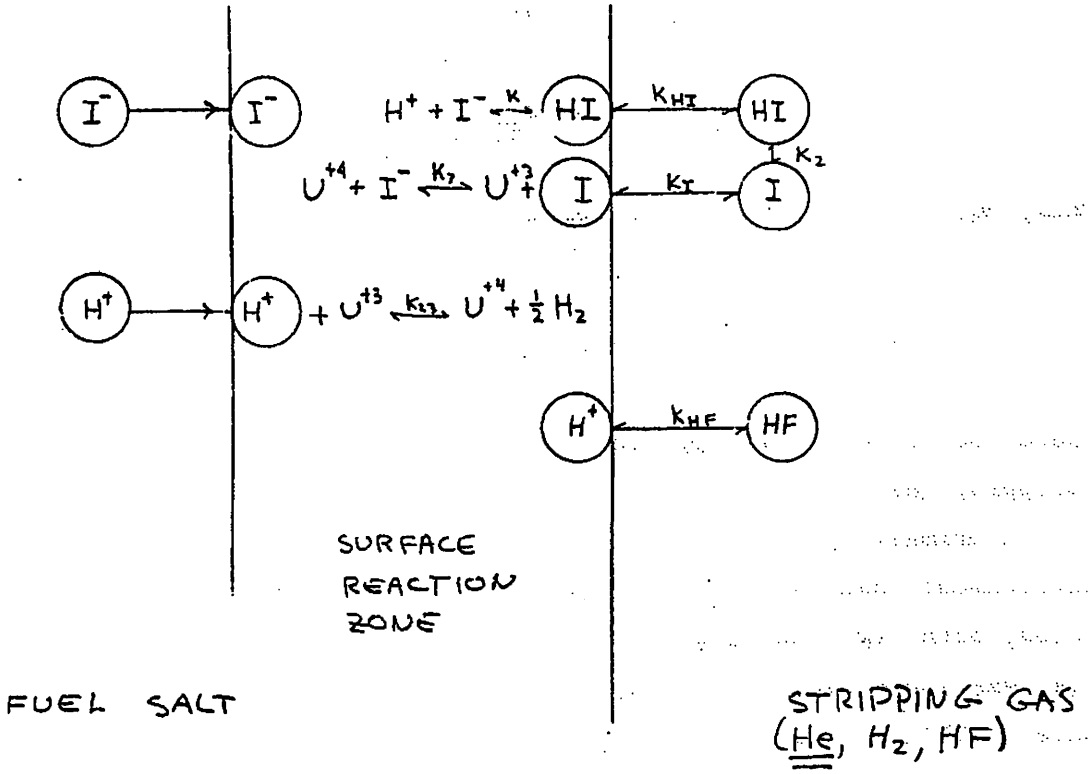

Fig. 7. Model for Iodide Desorption from Clean Fuel Salt.

$$P_{HI} = \frac{K'[I^-][H^+]}{K_{HI}}, \text{ and}$$

$$P_I = \frac{K_2 P_{HI}}{\sqrt{P_{H_2}}},$$

into Eq. (33) yields,

$$K_{eff} = \frac{K_{HI}}{K'[H^+]\left(1 + \frac{K_2}{\sqrt{P_{H_2}}}\right)}. \tag{39}$$

Alternatively, the expressions

$$P_{HI} = \frac{P_I}{K_2}\sqrt{P_{H_2}}, \text{ and}$$

$$P_I = \frac{K\zeta[I^-]U}{K_I},$$

may be substituted into Eq. (33) to yield a second expression for K_{eff},

$$K_{eff} = \frac{K_I}{K\zeta U\left(1 + \sqrt{\frac{P_{H_2}}{K_2}}\right)}, \tag{40}$$

The two expressions for K_{eff} given by Eqs. (39) and (40) are in fact completely equivalent, and despite the vast differences in value between K_9 and K_I on the one hand the ratio K'/K_{HI} on the other, both yield the same value for K_{eff}. This results because the two paths for iodine removal are not independent, but are in fact closely related by the requirement that all species are in equilibrium with each other. Thus the value of K_{eff}, as given by each expression, is simply a measure of tendency for the fuel composition to evolve I^- as HI(g) and I(g).

It is interesting to compare Eq. (39) with Eq. (36), which is the expression for K_{eff} appropriate for the laboratory tests. Note that K_{eff} is diminished by the factor $1/(1 + K_2/\sqrt{P_{H_2}})$ when helium carrier gas is employed instead of hydrogen. This factor represents the degree of dissociation of HI(g), which results in an effective reduction in solubility of HI(d) by removal of HI(g) from the scene.

The proper value for the partial pressure of hydrogen, which is required for estimation of K_{eff} from either expression, is not known at this time; therefore, this quantity will be treated as a parameter. If the main source of hydrogen in the primary system is inleakage from the source in the steam generator through the secondary system, it is guessed that the value of P_{H_2} will be rather low — in the range 10^{-8} to 10^{-6} atmospheres. Higher hydrogen pressures have the advantage of lowering the corrosion rate in the stripper. However, it is not known if addition of even small amounts of hydrogen to the stripping gas will be permissible due to consequent dilution of tritium and possible adverse effects of tritium control procedures.

2.4 Tentative Flowsheet for Iodine Removal

It is worthwhile to initially make some estimate of the degree of iodine removal that could be achieved by using a neutral stripping gas. Here "neutral" is used in the sense that equilibrium contact with the gas does not alter the oxidizing power of the fuel salt. As such, the contacting gas must contain some H_2 and HF.

2.4.1 Iodine Removal Using Neutral Stripping Gas

If it were possible to design an adequate iodine removal device utilizing an inert stripping gas, there would result the obvious advantage that no reducing contactor would be needed downstream from the stripper to return the fuel to its original oxidation state. It is clear that a large removal efficiency could not be achieved in a nonoxidizing stripper, but then a large efficiency is not needed. It should be recalled that the target iodine removal efficiency for a combined xenon plus iodine stripper is only 6%, which, together with a 63% xenon removal efficiency,

suffices to yield a 1/2% poison level with uncoated graphite. The bypass flowstream for this case is 8% of the primary flow rate.

The degree of iodine removal using inert stripping gas may be estimated as follows: Taking the fuel salt to be as oxidizing as permissible in the primary system, and assuming some value of P_{H_2}, the variation of which will be examined parametrically, the proton concentration in the fuel may be calculated from the value of K_{23}, the equilibrium constant for the reaction,

$$H^+ + U^{+3} \overset{23}{\rightleftharpoons} U^{+4} + 1/2\ H_2(g)\ .$$

K_{eff} may then be evaluated using Eq. (39), obtaining values for K_2' and K_1' at the given temperature from the constants given in Table 1. (Note K_1' is equivalent to K_{HI}/K'.) From K_{eff}, the ratio of gas to liquid flows required to achieve the required 6% stripping efficiency may be calculated by using Eq. (34). Finally, the partial pressure of HF which would render the gas neutral with respect to fuel salt may be estimated from $[H^+]$ and K_{HF} (K_0' in Table 1).

Table 3 lists some effective iodine solubilities and phase flow rates to yield a 6% iodine stripping efficiency for an assumed U^{+4}/U^{+3} ratio of 10^4. Values are given for t = 1300°F; poorer results are obtained at lower temperatures. We note reluctantly that the effective solubilities of iodine in contact with neutral stripping gas are quite high, necessitating use of excessive gas flows to achieve η_I = 6%. Thus, an oxidizing iodine stripper appears to be required, necessitating also the use of a reducing unit to return the fuel salt to its original oxidizing state.

2.4.2 Oxidizing Stripper for Xenon and Iodine Removal

We will now assume that the fuel salt is brought in contact with an oxidizing stripping gas to enhance the tendency for iodine removal. Protons for formation of HI in this case are provided by HF present in greater concentrations than in the previous section where neutral conditions were assumed. In addition to oxidizing iodide ion, the stripper will oxidize some portion of U^{+3} to U^{+4}; thus HF will be consumed and H_2 produced in the stripper.

Table 3. Values for K_{eff} and Q_g/Q_ℓ in a Nonoxidizing Stripper at Various Assumed Hydrogen Partial Pressures

Conditions: $U^{+4}/U^{+3} = 10^4$, t = 1300°F

P_{H_2} (atm)	P_{HF} (atm)	K_{eff} (g-mole/cc-atm)	Q_g/Q_ℓ for η_I = 6%
10^{-8}	3.3×10^{-6}	0.54	2600
10^{-6}	3.3×10^{-5}	0.49	2400
10^{-4}	3.3×10^{-4}	0.24	1100
10^{-2}	3.3×10^{-3}	0.041	200

Particular attention must be paid to the oxidizing power of the fuel leaving the stripper. It is necessary to assume that in this localized region of the primary system, the fuel is permitted to become more oxidizing than for the primary system as a whole. However, it is not clear how oxidizing it may be allowed to become. Most likely, Pa_2O_5 solubility effects would not play a role here since the greater oxidizing power of the fuel is not permanent, and any P_2O_5 induced to precipitate in the stripper will tend to redissolve in the reducing unit where the original oxidizing power is restored. Thus the sole limitation on maximum allowable U^{+4}/U^{+3} at the exit of the stripper is placed by the need to limit corrosion in that locale to acceptable levels. For the sake of being specific at this time, we will assume that the maximum oxidizing power at the exit of the stripping unit will be such that the equilibrium value of $[Ni^{+2}]$ will not exceed 10 ppm. This is a factor of 100 higher than permitted for the primary loop as a whole. It should be emphasized, however, that this is simply the equilibrium value and not the actual average Ni^{+2} content of the bypass flow in this region, since it is not likely that equilibrium would be attained throughout the liquid with such a limited contact with the wall.

Some computed results for various assumed stripping conditions are tabulated in Table 4. The first three columns are assumed conditions of temperature, hydrogen, and HF partial pressures. Values of P_{H_2} in the

Table 4. Computed Conditions for a Combined Xenon-Plus-Iodine Stripper Using an Oxidizing Stripping Gas

Assumed Conditions							
t	P_{H_2} (atm)	P_{H_2} (atm)	U^{+4}/U^{+3} at Stripper Exit	ℓSTP HF Consumed in Stripper/Sec	K_{eff} $\left(\frac{\text{g-mole}}{\text{cc-atm}}\right)$	Q_g/Q_ℓ for $\eta_I = 6\%$	PPM Ni^{+2} in Equilibrium with U^{+4}/U^{+3} at Exit of Stripper
1300°F (978°K)	10^{-8}	0.1	3×10^8	0.098	1.8×10^{-5}	0.086	62,000
		0.01	$\times 10^7$		$\times 10^{-4}$	0.86	620
1300°F (978°K)	10^{-6}	0.1	3×10^7	0.098	1.6×10^{-4}	0.78	620
		0.01	$\times 10^6$		$\times 10^{-3}$	7.8	6.2
1300°F (978°K)	10^{-4}	0.1	3×10^6	0.098	8.1×10^{-4}	3.9	6.2
		0.01	$\times 10^5$		$\times 10^{-3}$	39	0.062
1300°F (978°K)	10^{-2}	0.01	3×10^4	0.065	1.3×10^{-2}	65	6.2×10^{-4}
1050°K (839°K)	10^{-8}	0.1	1.2×10^{10}	0.098	4.7×10^{-5}	0.2	2.5×10^5
		0.01	$\times 10^9$		$\times 10^{-4}$	2.0	2500
1050°F (839°K)	10^{-6}	0.1	1.2×10^9	0.098	2.2×10^{-4}	0.9	2500
		0.01	$\times 10^8$		$\times 10^{-3}$	9.0	25
1050°F (839°K)	10^{-4}	0.1	1.2×10^8	0.098	5.2×10^{-4}	2.2	25
		0.01	$\times 10^7$		$\times 10^{-3}$	22	0.25
1050°F (839°K)	10^{-2}	0.1	1.2×10^7	0.098	5.8×10^{-4}	2.4	0.25
		0.01	$\times 10^6$		$\times 10^{-3}$	24	2.5×10^{-3}

range 10^{-8} to 10^{-6} may be anticipated from steam generator inleakage, whereas the higher values may be attained by deliberately adding H_2 to the stripping gas. For each temperature and P_{H_2}, HF partial pressures of 0.1 and 0.01 atmospheres were assumed.

The fourth column of Table 4 lists the values for U^{+4}/U^{+3} expected at the stripper outlet for the various assumed conditions. This may be computed from,

$$\left(\frac{[U^{+4}]}{[U^{+3}]}\right)_{\text{stripper outlet}} = \frac{K_{23}' \, K_{HF} \, P_{HF}}{\sqrt{P_{H_2}}} \qquad (41)$$

where the product $K_{HF} \, P_{HF}$ represents the proton concentration in the stripper. We note that the main advantage in higher H_2 partial pressures is lower U^{+4}/U^{+3} ratios at the stripper exit for a given value of P_{HF}. However, K_{23}' increases rapidly as the temperature decreases; hence the computed U^{+4}/U^{+3} ratio is quite a bit higher at the lower temperature.

The fifth column lists the rate at which oxidizer is consumed by its reaction with U^{+3}. This value, which is also twice the rate of hydrogen production, may be computed from the balance equation,

$$\frac{\text{g-mole}}{\text{sec}} \, U^{+3} \text{ oxidized to } U^{+4} = Q_\ell U_t \left(\frac{1}{U_2} - \frac{\sqrt{P_{H_2}}}{K_{23}' \, K_{HF} \, P_{HF}}\right), \qquad (42)$$

where U_t is the total uranium concentration of the fuel, U_2 the U^{+4}/U^{+3} ratio at the fuel inlet to the stripper, and Q_ℓ the liquid volumetric flow rate. For all cases except one the HF consumption rate is constant at 0.098 ℓSTP/sec since for all cases essentially all U^{+3} is converted to U^{+4} in the stripper.

The sixth and seventh columns list the values for K_{eff} and the required value for Q_g/Q_ℓ in order to attain 6% stripping efficiency for iodine. Here we note that high temperature and HF partial pressure enhances stripping while increased H_2 partial pressure has an inhibiting effect. The last column lists Ni^{+2} concentrations in the fuel which would

be in equilibrium with conditions assumed for each case. Here hydrogen has a beneficial effect in reducing Ni corrosion. It is interesting that lowering the temperature does not yield the expected benefit of lowering the rate of corrosion. This comes about because the reaction

$$U^{+3} + H^{+} \overset{23}{\rightleftharpoons} U^{+4} + 1/2\ H_2(g)$$

goes to the right with diminishing temperature, which more than compensates for the inhibiting tendency of lower temperatures on the corrosion reaction

$$2U^{+4} + Ni \rightleftharpoons 2U^{+3} + Ni^{+2}\ .$$

It is judged that the case indicated by the arrow in Table 4 represents the best compromise between required gas flows and nickel corrosion rates.

Note that 0.098 ℓSTP HF/sec are consumed in the stripper to oxidize the major portion of U^{+3} to U^{+4}. This amounts to 4.4×10^{-3} gmole/sec rate of HF addition. An equal reductant addition rate must be applied to the fuel salt somewhere in the primary system to maintain the U^{+4}/U^{+3} ratio at the desired level. This reduction step is a key feature in I-removal analyses from the MSBR and requires more detailed consideration than is given to it in this study. Summarized below are four possible approaches to the problem of adding reductant.

2.4.3 Reductant Addition for Maintenance of Initial U^{+4}/U^{+3} Ratio

1. Addition of Li°-Be°-Th°. If metallic lithium, beryllium, and thorium are dissolved in the fuel salt at the following rates,

gm/sec Li° = 0.014,

gm/sec Be° = 0.0041,

gm/sec Th° = 0.081,

the effect of HF addition in the I + Xe stripper is counteracted and the initial molar ratios of Li, Be, and Th are left unchanged. An equal rate of Li, Be, and Th must be removed from the fuel salt to maintain the initial concentration of uranium. This may be easily accomplished by tapping

the LiF, BeF_2, ThF_4 stream in the chemical processing facility. At this time recovery costs are higher than storage costs; hence under present circumstances, the metal added for reducing purposes would not be recovered. The incurred cost of reducing the fuel salt in this way would be the sum of the cost of the metal feed plus the added cost of waste storage.

2. Addition of Li°-Be°. The required rate of reductant addition may be achieved by addition of lithium and beryllium metal at the following rates:

gm/sec Li° = 0.021,

gm/sec Be° = 0.0061.

The above rates have the effect of maintaining the original molar ratio of Li to Be while reducing the concentrations of Th and U. However, the low rates of reactivity loss that are incurred make the scheme worth considering. It is estimated that reactivity will be lost at a rate of 6.1×10^{-6}-% δk/k per hr due to the above rates of Li° and Be° addition. This rate of reactivity loss would equal the worth of the control rods in about six years of reactor operation. The advantage of this scheme over the previous one is that no added waste storage costs are incurred. Also, the reductant feed is less expensive per unit time than when Li°-Be°-Th° are added.

3. Hydrogen Addition. This would have the virtue of achieving the required reduction with no added waste stream and with no alteration of fuel composition. A complete analysis of the feasibility of hydrogen addition, however, is a formidable task in itself, which is beyond the scope of this report. Experience in the Chemical Technology Division indicates that H_2 addition is not easily achieved, and may entail the use of contactors comparable in size to that required for I removal.

4. Addition of Zr°. Zirconium metal added at the rate of 0.1 gm/sec would achieve the required reduction rate. If left in the fuel this would be equivalent to adding a neutron poison of approximately 6.0×10^{-5}-% δk/k per hr, i.e., roughly the worth of the control rods in 208 days. Alternatively, Zr may be removed in the chemical processing facility. However, in so doing it is replaced by an equal number of equivalents of

Li + Be + Th, which must be discarded if the initial fuel composition is to be maintained. Thus when Zr is removed in the chemplant, methods 1 and 4 represent approximately equivalent processes.

2.4.4 Flowsheet for Xenon and Iodine Removal

A preliminary flowsheet for Xe + I removal is shown in Fig. 8 based on conditions in the stripper designated by the arrow in Table 4 and the means of fuel reduction designated as Case 1 in the above section.

No serious attempt has been made to calculate the heat source in the stripping gas system; however, if iodine is removed from the primary system at a rate equivalent to a one hr time constant, the heat load due to decay of iodine isotopes is estimated to be in the order of 3 MW. Since some unknown fraction of the bromine in the fuel will evolve with the iodine in the stripper, perhaps an additional 3 MW will accrue from that source as well. It is intended at this time merely to indicate that heat removal from stripping gas is necessary to maintain acceptable temperatures and that the heat removal rate is on the order of 6 MW.

The iodine evolved in the stripper will be in a highly reactive form – HI(g) and I(g) will react with all but the noblest of metals. Hence, it will probably not be possible to localize iodine adsorption in some designed chemisorption bed; nor would such appear to be desirable in view of the heat load on the bed that would have to be dissipated. Thus, the stripped iodine will most likely distribute generally on metallic surfaces throughout the gas system including the walls of the stripping unit where it will reside most likely as NiFI(c) until decay to xenon and subsequent evolution.

2.4.5 Required Stripping Gas Volume

The concentration of xenon in the stripping gas must be kept sufficiently low by decay or by xenon removal from the gas such that sufficient driving force for xenon removal from fuel salt is maintained in the stripper. How low is "sufficiently" low can only be determined by a cost optimization procedure that balances the incentives for a high xenon removal driving force, namely smaller stripping unit, lower liquid holdup, against the costs of achieving low xenon concentrations in the gas system.

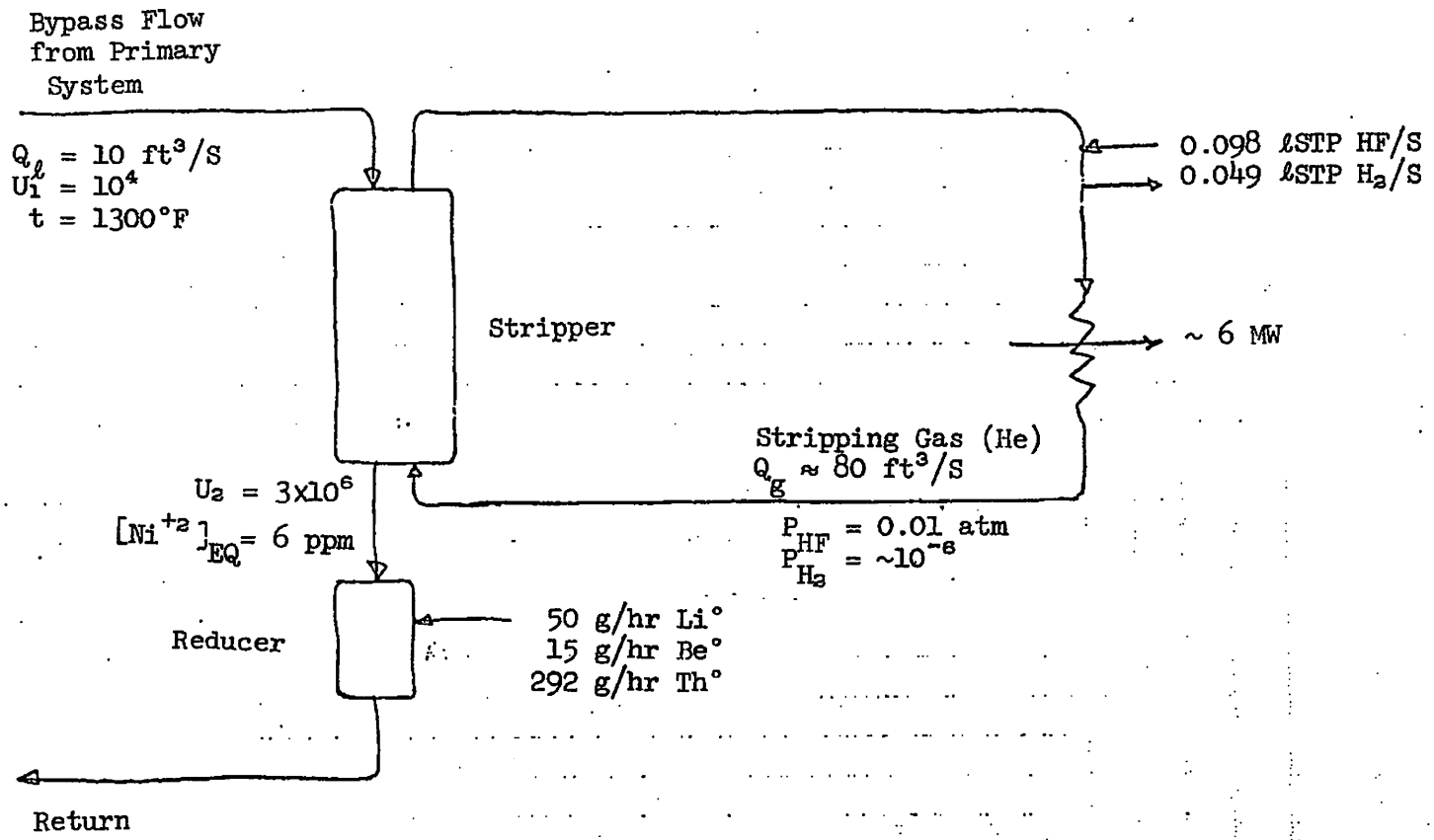

Fig. 8. Flowsheet for Combined Xenon and Iodine Removal. η_{Xe} = 62%, η_I = 6%.

Such a cost calculation can only be realistically attempted when the system design is much further along. However, in this regard the following considerations came to mind:

1. Since the stripping gas system must necessarily be large due to the large anticipated flows, unit sizes and interconnecting pipework, it appears to be logical to give prime consideration to ^{135}Xe decay as the principal means for xenon removal. Under these circumstances, xenon removal to charcoal beds would likely be quite expensive since the size of such beds is approximately proportional to the volumetric throughput, and substantially higher throughputs would be required than for the present MSBR reference design.

2. It has been judged that the off-gas system for the MSBR reference design is near optimum cost when the xenon concentration in the gas is maintained at 10% of the value which would be in equilibrium with the fuel salt at the desired 1/2% poison level.

3. When lower xenon concentrations in the gas phase are resorted to, it is possible that some highly advantageous stripping schemes become feasible — as will be more fully described in the following section. However, for a combined xenon-plus-iodine stripping device such as is presently considered, undoubtedly iodine stripping will be the limiting factor in the design, in which case there would be no advantage in maintaining extremely low xenon levels in the gas phase.

We thus tentatively conclude that the gas phase xenon concentration in the combined xenon-plus-iodine stripper be maintained at 10% of the equilibrium value existing at the 1/2% reactor poison level, and that ^{135}Xe decay be the principal method of removal from the gas system. A required gas system volume of approximately 4600 ft^3 may then be readily estimated, a value which applies to the case of uncoated graphite in the core. This is about equal to the present MSBR off-gas system volume including the drain tank, long delay and 48-hr recycle systems. Some key intermediate values in this calculation are given in Table 5.

Table 5. Computation of Required Gas Volume in a Combined Xenon-Plus-Iodine Stripper that Allows $[Xe]_g$ to be Maintained at 10% of the Equilibrium Value for 1/2% Poison Level and Uncoated Graphite

^{135}Xe production rate, g-mole/sec	7.14×10^{-6}
σ-135 at 1175°F, barns	1.01×10^{6}
λ-135, sec^{-1}	2.09×10^{-5}
g-moles ^{135}Xe in primary system at steady state with no removal; ~5% PF	0.025
$[^{135}Xe]_\ell$ in fuel salt assuming 95.7% resides in graphite[a] at 5% PF, g-mole/cc	2.2×10^{-11}
$[^{135}Xe]_\ell$ in fuel at 1/2% PF, g-mole/cc	2.2×10^{-12}
$[^{135}Xe]_g$ in equilibrium with $[Xe]_\ell = 2.2 \times 10^{-12}$ g-mole/cc	2.7×10^{-8}
10% of above $[Xe]_g$, g-mole/cc	2.7×10^{-9}
Required gas volume = production/$\lambda \cdot [Xe]_g$, ft^3	4600 ft^3

[a]See Section 3 of "Design Basis Report" by R. J. Kedl (to be published).

2.4.6 Flowsheet for Iodine Removal Alone

The above section pertains to a combined xenon-plus-iodine stripper where 8% of the primary flow is diverted to a stripper that removes 63% of the xenon and 6% of the iodine throughputs sufficient to accomplish the objective of 1/2% poison level. An alternative scheme would divert a smaller bypass flow through a device that would be primarily an iodine stripper, though it would also remove essentially all of xenon throughput. Some supplementary xenon-removal method would be required in this case to reduce the neutron poison to the desired level since the lowest possible leve with iodine removal alone is about 0.9%. Though the combined xenon-plus-iodine stripper seems at this time to be the more advantageous scheme,* the iodine stripper concept has the inherent advantage of requiring a smaller liquid throughput. Thus the required reductant addition rate is correspondingly lower, as is probably also the liquid holdup in the stripper unit as compared with requirements for Xe + I removal.

*This view is no longer held. See Summary.

As indicated in the Introduction, an iodine stripper that accepts a bypass flow equal to 0.8% of the primary and removes 60% of the iodine throughput would capture the bulk of the ^{135}I born in the reactor before it can decay to ^{135}Xe. Thus the iodine stripper has 1/10 the liquid flow and approximately 10 times the iodine efficiency of the combined xenon-plus-iodine device. The required reductant addition rate therefore is 1/10 the value shown in Fig. 8 for the combined Xe + I removal scheme.

If the same gas composition is used in the iodine stripper as was selected for the I + Xe removal case where only 6% iodine removal efficiency was required, then in order to achieve the 60% efficiency desired for iodine removal alone the relative gas flowrate must be increased. The factor of 10 increase in efficiency may be achieved by increasing the relative gas flow by the same factor. However, since the liquid stream is now only 1/10 as large, the absolute value of the stripping gas flow is the same for the two cases.

Thus we arrive at the tentative flowsheet for iodine removal alone shown in Fig. 9. The gas system is identical with that shown in Fig. 8 for combined Xe + I removal while liquid feed and reductant addition rates are 1/10 as high.

2.5 Iodine Transport to Graphite

We will now attempt to verify the assumption, which has thus far been implied, that iodine transport to even uncoated graphite will not be a significant factor in determining the ^{135}Xe poison level in the MSBR.

Iodine may enter the graphite as HI(g) or I(g) formed at the graphite boundary by the reactions,

$$H^+ + I^- \rightleftharpoons HI(g) \text{ , or} \qquad (43)$$

$$U^{+4} + I^- \rightleftharpoons I(g) + U^{+3} \text{ .} \qquad (44)$$

Additionally, the vaporization of volatile halides may play a role in iodine transport into the graphite.

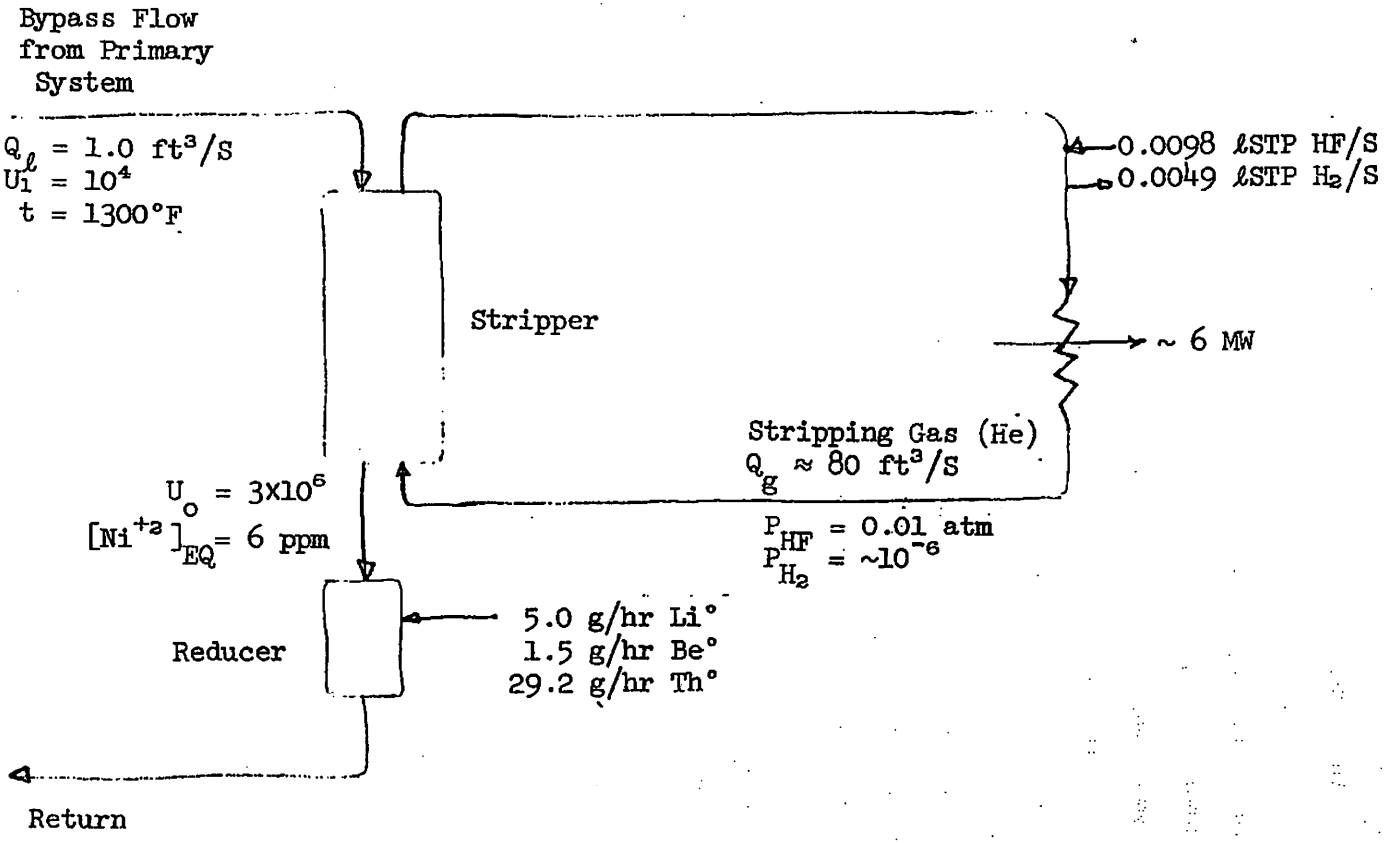

Fig. 9. Flowsheet for Iodine Removal Alone.

2.5.1 Iodine in Graphite as HI(g) and I(g)

From the definition of K'_{11} in Table 1 we may write the expression for $[HI]_G$, the concentration of HI in the graphite pores which is in equilibrium with $[I^-]$ and $[H^+]$, the iodide and proton concentrations in the fuel, via oxidation reaction Eq. (43),

$$[HI]_G = \frac{[H^+][I^-]}{K'_{11}\,RT} . \tag{44}$$

The proton concentration is a function of the U^{+4}/U^{+3} ratio in the melt (written below as U) and whatever value is the effective partial pressure of hydrogen. Thus,

$$[H^+] = \frac{\sqrt{P_{H_2}}\,U}{K'_{23}} \tag{45}$$

where the equilibrium constant, K'_{23}, pertains to the reaction,

$$H^+ + U^{+3} \overset{23}{\rightleftharpoons} U^{+4} + 1/2\ H_2(g) , \tag{46}$$

and is defined by,

$$K'_{23} \equiv \frac{\sqrt{P_{H_2}}\,U}{[H^+]} . \tag{47}$$

The dependence of K_{23} on temperature may be determined from Table 1 by combining reactions (12) and (13) to yield

$$K_{23}(T) = 1.11 + 8.02\,\frac{(10^3)}{T} \tag{48}$$

If we now conservatively assume that the entire graphite pore volume, V_G, contains the concentration $[HI]_G$, which is in equilibrium with fuel volume, V_ℓ, combining Eqs. (44) and (45) leads to,

$$\frac{V_G[HI]}{V_\ell[I^-]} = \frac{\sqrt{P_{H_2}}\, U}{K_{23}\, K_{11}\, RT} \frac{V_G}{V_\ell} . \qquad (49)$$

However, at low values of P_{H_2} most of the HI(g) dissociates to I(g), where the concentration, $[I]_G$, is given by,

$$[I]_G = \frac{K_2[HI]_G}{\sqrt{P_{H_2}}} . \qquad (50)$$

Combining Eqs. (49) and (50) yields the desired result,

$$\frac{V_G\left([HI]_G + [I]_G\right)}{V_\ell[I^-]} = \left(\sqrt{P_{H_2}} + K_2\right) \frac{U}{K_{11}\, K_{23}\, RT} \cdot \frac{V_G}{V_\ell} , \qquad (51)$$

where the ratio on the left is the iodine content of the graphite as I(g) and HI(g) relative to the total iodine contained in the fuel. Values of this ratio are given in Table 6 for several assumed hydrogen partial pressures. The pore volume, V_G, was taken to be 570 ft^3, which is 10% of the total graphite volume. The fuel was assumed to be as oxidizing as permissible in the primary circuit, and the temperature 1175°F (908°K).

Table 6. Ratio Iodine in Graphite as HI(g) + I(g) to Iodine in Fuel Salt Assuming Interphase Equilibrium as Per Eq. (51)

Conditions: T = 908°K
Graphite porosity = 10%
$U^{+4}/U^{+3} = 10^4$

Hydrogen Partial Pressure (atm)	Iodine in Graphite as HI + I / Iodine in Fuel
10^{-8}	1.1×10^{-6}
10^{-6}	1.3×10^{-6}
10^{-4}	3.8×10^{-6}

In fact there will be far less iodine in the graphite than indicated in Table 6 because of the time required for diffusion into the interior pores. ^{135}I decays as it diffuses, hence the equilibrium concentration will not be reached. Some idea of the ratio of actual ^{135}I [as I(g)and HI(g)] to equilibrium content of graphite may be ascertained from the calculated ^{135}Xe distribution between fuel and graphite given by R. J. Kedl.* For uncoated graphite at infinite removal time the ratio is given as:

$$\frac{^{135}\text{Xe in graphite}}{^{135}\text{Xe in fuel}} = \frac{4.8}{0.086} = 56 .$$

The equilibrium ratio may be computed from

$$\frac{^{135}\text{Xe in graphite}}{^{135}\text{Xe in fuel}} = \frac{V_G}{V_\ell} \frac{1}{K_{Xe} RT} = 1.3 \times 10^3 ,$$

which is obtained by using $K_{Xe} = 3.5 \times 10^{-9}$ g-mole/cc-atm at T = 908°K (1175°F). Thus the actual to equilibrium ratio for ^{135}Xe is $56/1.3 \times 10^3$ or 4.3%. Assuming HI and I diffuse about as rapidly as Xe, the actual iodine content should be somewhat lower since ^{135}I decays more rapidly than ^{135}Xe. We may thus conclude that the ^{135}I content of the graphite (as HI and I) will be about a factor of 30 lower than the equilibrium values given in Table 6, which brings the ratio of I in graphite to I in fuel down to about 4×10^{-8} for $P_{H_2} < 10^{-6}$ atm.

2.5.2 Iodine in Graphite Due to Halide Volatility

It may at first appear strange that volatility effects need to be considered at primary loop temperatures; however, observation of the values given in Table 7 for the vapor pressures of some pure halides at 1000°K indicates that this is indeed the case.[7,8] Some rather volatile iodides may be formed in MSBR fuel.

---

*Report to be published.

Table 7. Vapor Pressures of Some Pure Halides at 1000°K

Halide	Vapor Pressure at 1000°K (mm Hg)	Source
ZrI_4	2.3×10^5	a
BeI_2	12,000	b
BeFI	100	c
LiI	2.5	d
$BeBr_2$	9300	e
LiBr	0.62	d

a – Ref. 7 for $ZrI_4(s)$, extrapolated from s.p., 772°K.

b – Ref. 7, extrapolated from b.p., 760°K.

c – Calculated from ΔG_f^o for $BeI_2(g)$ and $BeF_2(g)$ given in Ref. 8. See text.

d – Calculated from ΔG_f^o data given in Ref. 8.

e – Ref. 7, extrapolated from b.p., 803°K.

The partial pressure developed by a particular specie dissolved in the melt depends not only on its inherent volatility but also by the concentration of ions that form the molecule, and the extent to which it is bound by the liquid. For example, consider the case of BeI_2 which may be thought of as evolving in two steps,

$$Be^{+2} + 2I^- \overset{1}{\rightleftharpoons} BeI_2(d) \overset{2}{\rightleftharpoons} BeI_2(g) , \qquad (42)$$

where step 1 symbolically represents the probability that two iodide and one beryllium ions exist adjacent to one another, while the extent to which step 2 proceeds depends on the volatility of BeI_2 and the degree to which it is bound in the liquid. For step 1,

$$K_1 = \frac{X_{BeI_2(d)}}{\left(X_{Be^{+2}}\right)\left(X_{I^-}\right)^2} . \tag{43}$$

For step 2,

$$K_2 = \frac{P_{BeI_2}}{\left(\gamma_{BeI_2}\right)\left(X_{BeI_2(d)}\right)} . \tag{44}$$

Combining Eqs. (43) and (44) yields,

$$K_1 K_2 = \frac{P_{BeI_2}}{\left(\gamma_{BeI_2}\right)\left(X_{Be^{+2}}\right)\left(X_{I^-}\right)^2} , \tag{45}$$

where the product $K_1 K_2$ may be identified with the vapor pressure of pure $BeI_2(\ell)$, $P^{o}_{BeI_2(\ell)}$. Hence, the partial pressure of dissolved BeI_2 may be written,

$$P_{BeI_2} = \left(\gamma_{BeI_2}\right)\left(X_{Be^{+2}}\right)\left(X_{I^-}\right)^2\left(P^{o}_{BeI_2(\ell)}\right) . \tag{46}$$

Since the value of X_{I^-} is estimated to be about 8×10^{-9} with iodine being stripped at a rate equivalent to a 1-hr removal time, it is clear that the necessity that two iodide ions meet to form BeI_2 drastically reduces its anticipated partial pressure. Similarly, the anticipated partial pressure of ZrI_4, which is inherently highly volatile, will be vanishingly small since five fission product ions must come together, the probability of this occurrence being given by $(X_{Zr^{+4}})(X_{I^-})^4$.

We will thus assume that the iodides which most likely possess significantly high partial pressures are the ones that contain only one fission product atom. This restricts our interest to LiI and BeFI for the present.

We will again conservatively assume that the graphite pore space is in equilibrium with the fuel salt with respect to the distribution of LiI and BeFI, in which case we can write the ratio,

$$\frac{\text{g-moles LiI + BeFI in graphite}}{\text{g-moles } I^- \text{ in fuel}} =$$

$$\frac{(\gamma_{LiI})(X_{Li^+})(X_{I^-})(P^{\circ}_{LiI}) + (\gamma_{BeFI})(X_{Be^{+2}})(X_{I^-})(P^{\circ}_{BeFI})}{X_{I^-} - \frac{V_\ell}{V_1}} \cdot \frac{V_G}{RT} , \quad (47)$$

where V_1 has the value of 20 cc/g-mole of fuel. Note that X_{F^-}, the fraction of anions that are F^-, is taken as 1. Data presented by Smith, Ferris, and Thompson[9] and by Hitch and Baes,[10] and calculations by Baes[11] indicate that the activity coefficient for BeF_2 is 0.15 for a fuel of approximately MSBR reference composition. We will therefore assume that also $\gamma_{BeFI} = \gamma_{BeF_2} = 0.15$. Values for γ_{LiF} are estimated to be 0.5 and we will assume this value for γ_{LiF}. Rewriting Eq. (47) yields,

$$\frac{\text{g-mole LiI + BeFI in graphite}}{\text{g-mole } I^- \text{ in fuel}} =$$

$$(\gamma_{LiI} X_{Li^+} P^{\circ}_{LiF} + \gamma_{BeFI} X_{Be^{+2}} P^{\circ}_{BeFI}) \frac{V_G}{V_\ell} \cdot \frac{V_1}{RT} . \quad (48)$$

The value of P°_{LiF} at 1000°K may be obtained from the relation

$$\ell n\ P^{\circ}_{LiF} = - \frac{\Delta G^{\circ}_{50}}{RT} , \quad (49)$$

where ΔG°_{50}, the free energy change for the reaction

$$LiI(\ell) \rightleftharpoons LiI(g) , \quad (50)$$

may be obtained directly from the JANAF tables.[8] Similarly, P°_{BeFI} is obtained from

$$\ell n\ P_{BeFI} = - \frac{\Delta G^{\circ}_{52}}{RT} , \quad (51)$$

where ΔG°_{52} is the free energy change for the reaction

$$1/2\ BeF_2(\ell) + 1/2\ BeI_2(\ell) \rightleftharpoons BeFI(g)\ . \qquad (52)$$

Since the specie BeFI(g) is not listed in the JANAF tables, its free energy of formation was estimated as being the average of free energies of formation of $BeF_2(g)$ and $BeI_2(g)$ which are listed.* This procedure yields $\Delta G_f^\circ = -116.115$ kcal/g-mole for BeFI(g) at 1000°K which, together with ΔG_f° data given for $BeF_2(\ell)$ and $BeI_2(\ell)$, yields the value for P°_{BeFI} given in Table 7.

Substituting the known values into Eq. (48) yields:

$$\frac{\text{g-mole (LiI + BeFI) in graphite}}{\text{g-mole } I^- \text{ in fuel}} = 4.5 \times 10^{-7} \qquad (53)$$

in which the ratio LiI(g)/BeFI(g) is about 3/4.

Thus we may conclude that volatile iodides do not move into the graphite in sufficient quantity to significantly affect the estimation of the ^{135}Xe poison level. It is interesting, however, to compare Eq. (53) with values given in Table 6 for the distribution of iodine as HI(g) and I(g) between fuel and graphite. Of the iodine that does enter the graphite, approximately 1/6 does so by volatility of LiI and BeFI.

3. XENON AND IODINE STRIPPER DESIGN

3.1 Design Theory for Henry's Law Gas of Arbitrary Solubility

In the previous section it was shown that the total partial pressure exerted by the volatile iodine species HI and I may be directly related to the iodide concentration in the melt via the factor $1/K_{eff}$, where the solubility coefficient, K_{eff} (g-moles/cc-atm), depends on the chemical environment according to Eq. (39) or Eq. (40). Thus, this situation has the formalism of a Henry's Law gas, and the stripping theory developed

---

*This approximation was checked for BeFCl(g) at 1000°K with the following result: $\Delta G_f^\circ = -142.514$ (tabulated).
$\Delta G_f^\circ = -140.876$ (average of ΔG_f° for BeF_2 and $BeCl_2$).

for that case (e.g., see Coulson and Richardson[12]) may be applied, so long as it may be assumed that K_{eff} is constant throughout the stripper. This theory will be reviewed briefly here since there are a number of interesting implications for iodine stripping.

It will be convenient first to have an expression for Q_{go}, the minimum volumetric flow of stripping gas required for a particular stripping efficiency, η, and liquid throughput, Q_ℓ. Referring to Fig. 10, an iodine mass balance may be written,

$$Q_g[I_g]_2 = \eta_I Q_\ell [I^-]_2 \tag{54}$$

where the lean gas is assumed to be completely devoid of iodine, the subscript 2 refers to the rich end of the stripper, and the symbol $[I_g]$, signifies the total concentration of gaseous iodine as HI and I. The minimum gas flow would occur when the gas and liquid phases at the rich end are in equilibrium; i.e., when

$$P_I = \frac{[I^-]}{K_{eff}} \tag{55}$$

where P_I represents the sum of HI and I partial pressures. In this case,

$$[I_g]_2 = \frac{P_I}{RT}, \tag{56}$$

which, when substituted into Eq. (54), yields the minimum gas flow rate,

$$Q_{go} = \eta_I K_{eff} RT \cdot Q_\ell . \tag{57}$$

Flows of Q_{go} are required for equilibrium. However, if infinitely large contactors are to be avoided, gas flows must exceed Q_{go}. Alternatively, it may be said that when $Q_g = Q_{go}$, the number of transfer units, N_L, is equal to infinity; as Q_g increases above Q_{go}, the number of transfer units of separation decreases.

We will now derive the relation between Q_g and N_L. Referring to Fig. 10, we may equate the loss of iodide from the liquid flow across the

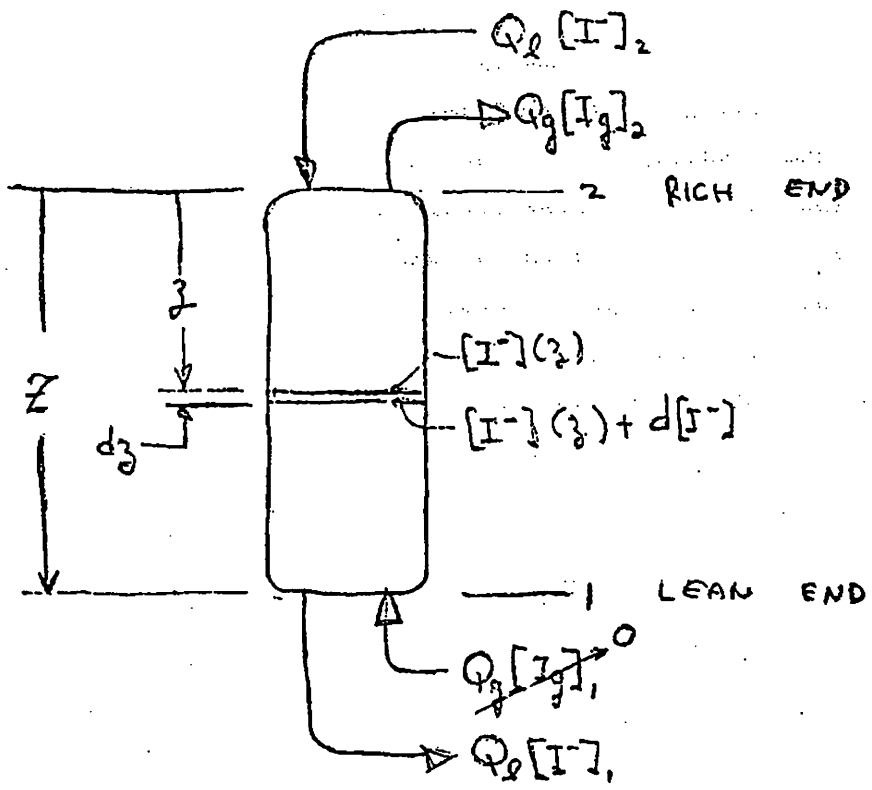

Fig. 10. Flow Schematic for Countercurrent Stripper.

differential distance, dz, to the rate of iodide transport to the surface of the liquid. Thus, if resistance to transfer resides primarily in the liquid,

$$k_L a \left([I^-] - [I^-]^* \right) A \, dz = - Q_\ell d \, [I^-] \, . \tag{58}$$

Equation (58) applies particularly to a packed column, but with minor changes the following development may be applied to any counter-current contactor. The quantity "a" is the packing surface area per unit volume of column, and "A" is the cross-sectional area of the column. k_L is the mass transfer coefficient which is completely equivalent to h_m used in other portions of this report; however, k_L is traditional for packed columns. $[I^-]$ is the bulk liquid concentration of iodide at elevation z and $[I^-]^*$ is the value of $[I^-]$ at the liquid-gas interface. Rearrange and integrate over the length of the column, Z;

$$Z = \frac{Q_\ell}{k_L \, a \, A} \int_{[I^-]_1}^{[I^-]_2} \frac{d[I^-]}{[I^-] - [I^-]^*} \, . \tag{59}$$

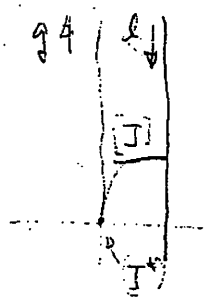

The factor,

$$H_L \equiv \frac{Q_\ell}{k_L \, a \, A} \tag{60}$$

is termed the height of a transfer unit, while the integral,

$$N_L \equiv \int_{[I^-]_1}^{[I^-]_2} \frac{d[I^-]}{[I^-] - [I^-]^*} \, , \tag{61}$$

is the so-called number of transfer units – the value of which indicates the degree of separation. Note that for a highly insoluble gas and liquid film controlling, $[I]^*$ goes to zero, which results in

$$N_L = \ell n \frac{[I]_2}{[I]_1} \, . \tag{62}$$

When there is significant gas solubility an expression for $[I^-]^*$ may be obtained from an iodine mass balance over the bottom end of the columns. The gas phase iodine concentration at elevation, z, given by,

$$[I_g](z) = \frac{Q_\ell}{Q_g}\left([I^-](z) - [I^-]_1\right), \tag{63}$$

is in equilibrium with $[I^-]^*(z)$, the liquid surface concentration at that elevation. Hence,

$$[I^-]^*(z) = K_{eff}\,[I_g](z)\,RT\,, \tag{64}$$

and

$$[I^-]^*(z) = K_{eff}\,RT\left([I^-](z) - [I^-]_1\right)\frac{Q_\ell}{Q_g}\,. \tag{65}$$

Substituting Eq. (65) into (61) and integrating yields after rearranging,

$$N_L = \frac{1}{1 - (Q_{go}/Q_g)/\eta_I}\,\ell n\left(\frac{1 - (Q_{go}/Q_g)}{1 - \eta_I}\right) \tag{66}$$

where Q_{go} is the minimum gas flow requirement given by Eq. (57). It may be shown that the value of N_L when $Q_{go}/Q_g = \eta_I$, which is indeterminate in Eq. (66), is given by

$$N_L\,(Q_{go}/Q_g \to \eta_I) = \frac{\eta_I}{1 - \eta_I}\,. \tag{67}$$

For infinite stripping gas flow,

$$N_L\,(Q_{go}/Q_g = 0) = -\,\ell n\,(1 - \eta_I)\,, \tag{68}$$

which is equivalent to the expression given in Eq. (62) for the case of a highly insoluble gas.

N_L is plotted in Fig. 11 vs the ratio Q_{go}/Q_g for three values of the stripping efficiency. Most noteworthy is the observation that when only small stripping efficiencies are called for, as in our case for iodine in the combined Xe + I stripper, stripping gas flows only slightly in excess of equilibrium requirements serve to dramatically reduce the value of N_L. Thus, to achieve 6% iodine stripping in the Xe + I stripper which would as indicated in Table 4 call for an equilibrium flow of

$$\frac{Q_{go}}{Q_\ell} = 7.8$$

at our selected design conditions, we may be increasing the gas flow to only

$$\frac{Q_g}{Q_\ell} = 8.1$$

reduce the number of transfer units of separation to

$$N_L = 0.2 \ .$$

The implication is that this is a quite small degree of separation and could be easily achieved by almost any reasonable contact.

For the case of iodine stripping alone an efficiency of 60% was tentatively selected, operating on a liquid throughput of one-tenth that contemplated for the combined Xe + I stripper. If the chemical environments are the same for both cases, i.e., equal values for K_{eff}, then for iodine stripping alone equilibrium demands,

$$\frac{Q_{go}}{Q_\ell} = 78 \ .$$

Equation (66) and Fig. 11 show that increasing the gas flow by 20%, i.e., to

$$\frac{Q_g}{Q_\ell} = 93.6 \text{ at } \frac{Q_{go}}{Q_g} = 0.8 \ ,$$

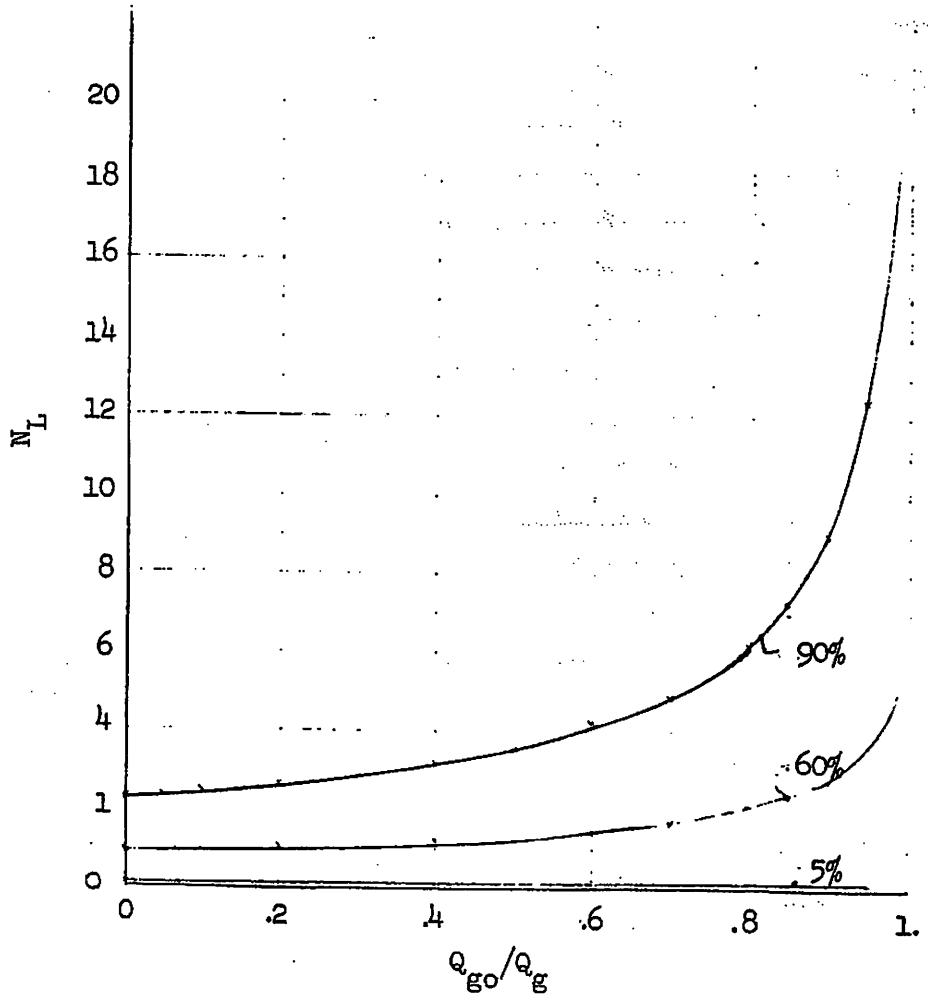

Fig. 11. Number of Transfer Units vs the Ratio Q_{go}/Q_g For Various Stripping Efficiencies.

[Eq. (66)]

serves to reduce the required degree of separation to

$$N_L = 2 .$$

In summary, the combined Xe + I stripper requires one transfer unit of xenon separation and 0.2 transfer unit of iodine separation to carry out the objective of 63 and 6% xenon and iodine removal, respectively. For iodine stripping alone we may anticipate a requirement of ~2 transfer units to obtain the desired 60% stripping efficiency. These all represent rather modest degrees of separation, which could be attained by almost any type of contactor. Hence, selection of the type of contactor may freely be made on the basis of its other desirable characteristics — low liquid holdup and low gas pressure drop possibly being the two most important.

The following sections describe some speculative stripper designs for these two cases. The word speculative must be emphasized. It is merely intended to show that there are a number of design approaches that offer reasonable opportunity for achieving the desired separations in a fashion that may be acceptable for the MSBR primary loop. Almost all stripping experience has been with aqueous solutions, and many of the empirical equations used to design these units implicitly assume water solution physical properties. Hence, this body of knowledge may be applied to molten salts, which have about ten times the viscosity and twice the surface tension of water, only with a good deal of caution and skepticism.

3.2 Spray Desorption

Spray columns are worthy of consideration because in general they are low holdup and low gas pressure drop devices. They are not appropriate when a high degree of separation is required; however, as indicated in the previous section, only modest separations are required for the cases considered here.

There exist at least three mechanisms for desorption from droplets in a spray column: (1) mass transfer from more or less quiescently falling droplets in the gas stream, (2) accelerated desorption during and immediately after droplet formation, and (3) flashing desorption that occurs

when the vapor pressure of the droplet exceeds the gas pressure. Each of these mechanisms requires some discussion.

3.2.1 Mass Transfer from Falling Drops

This is usually presumed to be the principal mechanism for mass transfer in conventional spray columns. The equation for counterflow stripping derived in the previous section applies with an altered definition for H_L. If one assumes uniformly sized droplets of diameter, d_p, falling with velocity u_p, it may be shown from Eq. (60) that

$$H_L = \frac{d_p u_p}{6 k_L} . \tag{69}$$

If we asume the gas velocity to be small compared with the terminal velocity of the drop, and use an appropriate correlation for k_L, e.g.,

$$Sh = 2.0 + 0.57 Re_p^{0.5} Sc^{0.35} \tag{70}$$

given by Griffith,[13] the values of H_L obtained as a function of d_p are given in Table 8. Thus, it may be observed that to obtain a reasonable tower size by means of this transfer mechanism, droplet sizes need to be quite low – on the order of 0.01 cm.

However, all of this is largely academic since spray towers do not behave in this fashion. The rate of droplet agglomeration is high in spray towers, hence we could expect the effectiveness for mass transfer to diminish rapidly with distance from the liquid inlet. (Note from Table 8, H_L varies about as d_p^2 in the intermediate regime and even more rapidly in the Stokes' regime.) Also, spray tower data[14] show a strong dependence of H_L on liquid flow rate which should not occur if this mechanism dominates – Q_ℓ does not appear in Eq. (69).

Finally, the maximum liquid loading per unit area of the spray tower appears to be approximately[14] 0.0045 $ft^3/sec\text{-}ft^2$. Hence a minimum tower diameter of ~55 ft would be needed to accommodate the 10-ft^3/sec liquid flow required for Xe + I stripping, while the minimum diameter for iodine stripping would still be a rather large 18 ft.

Table 8. Hypothetical Height of a Transfer Unit of a Spray Tower as Function of Droplet Size Per Eqs. (69) and (70)

Based on mass transfer in free fall only

Drop Size (cm)	Terminal Velocity (cm/sec)	Re_p	H_L (ft)
0.01	42[a]	0.05	0.5
0.1	1670[b]	19	200
0.2	3690[b]	83	850
0.3	5860[b]	200	2000

[a] Stoke's regime.

[b] Intermediate regime.

Assumed physical properties:

$\rho_\ell = 3.3$ g/cc
$\rho_g = 4.9 \times 10^{-5}$ g/cc
$\mu_g = 4.3 \times 10^{-4}$ g/cm-sec
$S_g = 1750$
$D_\ell^c = 1.3 \times 10^{-5}$ cm^2/sec

It is therefore concluded that stripping by means of the mechanism of mass transfer from free falling droplets is not a desirable objective.

3.2.2 Mass Transfer During and Soon After Droplet Formation — Spray Desorption

There is a small body of literature devoted to the study of mass transfer from newly formed droplets with a recent summary given by Rajan and Heidegar.[15] Evidently mass transfer coefficients may be as much as an order of magnitude higher near the inlet nozzle compared with an identical droplet in quiescent fall. The accelerated transfer rate is due to transient hydraulic disturbances in the droplet brought about by the shearing action during formation. In addition, the region near the inlet nozzle of a spray tower is important because it contains the smallest drop sizes. Hence, the term "spray desorption" signifies an accelerated

mass transfer mechanism from droplets near the inlet nozzle due both to mixing within the droplet and as a consequence of small droplet size.

The theory governing spray desorption has not yet been translated into practical design formulae; however, seawater deoxygenation data summarized by Eissenberg and Spiewak[16] indicate that from two to three transfer units of separation may be achieved by this mechanism using a "low pressure" inlet nozzle. The data are summarized in Table 9. High ΔP, atomizing sprays, achieved up to nine transfer units of separation, which is equivalent to 99.99% efficiency for oxygen stripping.

Table 9. Number of Transfer Units of Water Deoxygenation Achieved by "Spray Desorption" (see Ref. 16)

Water Temperature (°F)	Inlet Nozzle Type	Number of Transfer Units of Separation
50	"Low pressure"	2.2
100	"Low pressure"	2.6
200	"Low pressure"	3.0
300	"Low pressure"	3.3
~50	"Atomizing spray," increasing ΔP across nozzle	3.7 (to a maximum of)
~50	"Atomizing spray," increasing ΔP across nozzle	~9

One would like to have more detail on nozzle design, droplet size, ΔP across nozzle, etc., accompanying the data given in Table 9, but unfortunately this is not available. Hence, we may only conclude that approximately two transfer units of iodine or xenon stripping could likely be expected by means of spray desorption without excessively demanding conditions at the inlet nozzle.

3.2.3 Flashing Desorption

This also occurs near the inlet nozzle when the sudden drop in liquid pressure brings the hydraulic pressure in the droplet well below the liquid vapor pressure. Eissenberg and Spiewak[16] summarize the results of tests for seawater deoxygenation. It was found that full equilibrium exchange, which ranged from seven to eight transfer units, was achieved in some scattered tests, while approximately four transfer units are typical for tests conducted with some care in nozzle selection and sealing of the apparatus. More or less crudely run field tests generally attained approximately two transfer units of separation by means of flashing desorption.

The pressure drops through the spray nozzles ranged from 1 to 20 psi. The atomizing nozzles used for the higher pressure drops were not found to be superior to the lower pressure drop, nonatomizing nozzles. Neither was the degree of separation found to be a sensitive function of the fraction of liquid evaporated in the flashing range tested, 0.1 to 0.8%.

Fuel salt, of course, will not flash downstream from the nozzle. Hence, this mechanism probably does not apply to iodine or xenon stripping. However, flashing conditions with fuel salt could in some degree be approached by saturating the melt with helium upstream from the nozzle. If helium saturation at 200 psi pressure is achieved, dropping the pressure rapidly to atmospheric will "flash" off a volume of helium equal to ~0.1% of the amount of seawater leaving as vapor on the above cited deoxygenation tests. The degree of iodine or xenon stripping achieved thereby is not known.

Hence, we can come to the following conclusions regarding the use of spray columns for iodine or xenon stripping.

1. We should primarily strive for the "spray desorption" mechanism by which we may reasonably count on two transfer units of separation. This is adequate for either the iodine + xenon stripper or the iodine stripper cases.

2. There is no incentive for attempting to achieve a significant amount of stripping by means of mass transfer from quiescently falling drops.

3. Saturation with helium upstream from the nozzle (or even inclusion of helium bubbles) in order to simulate flashing desorption is worth considering, but the degree of transfer so achieved cannot be predicted.

We are therefore led to the spray desorption concept indicated schematically in Fig. 12. Tables 10 and 11 list some design characteristics for the two cases of interest.

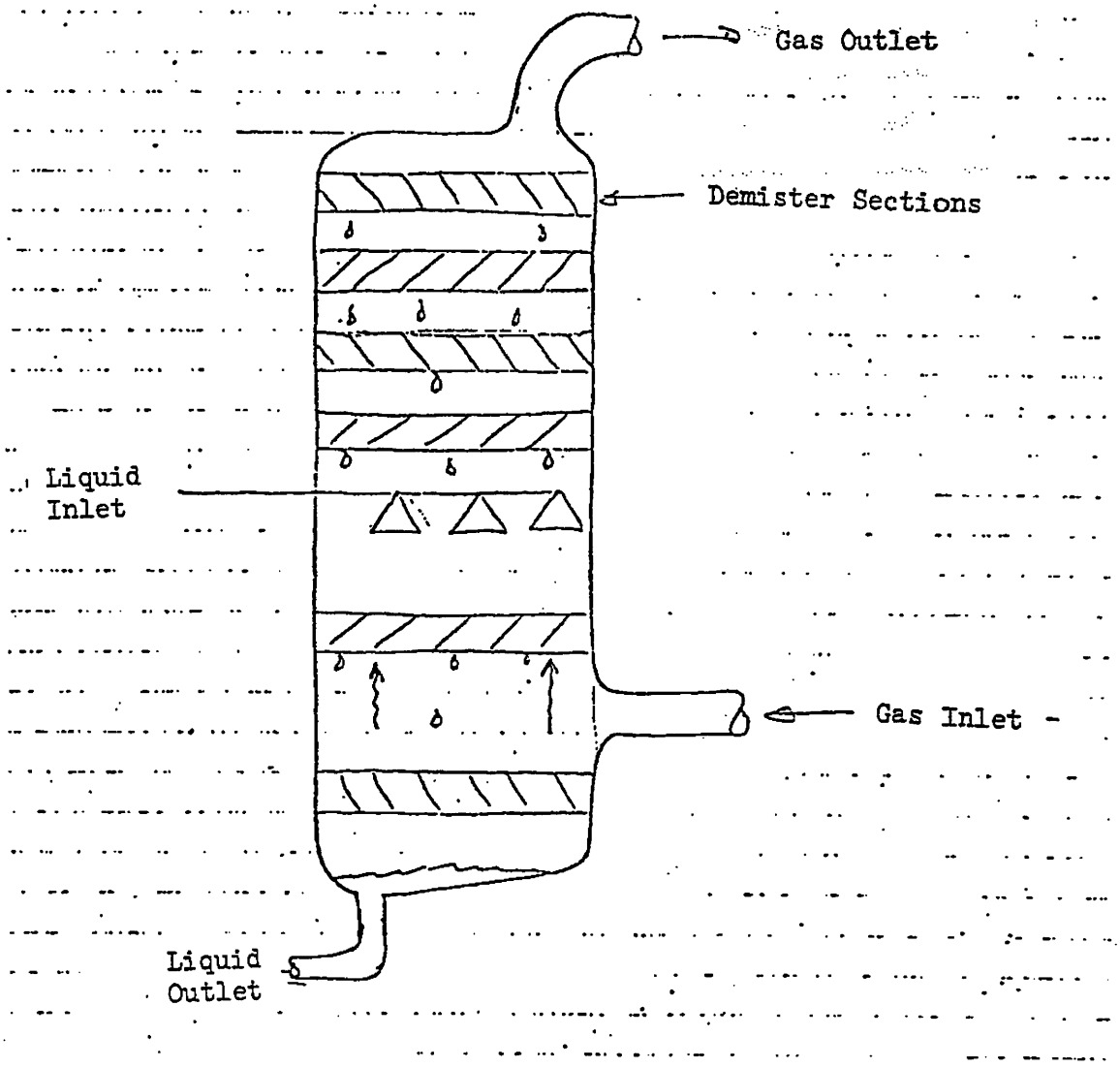

Fig. 12. Spray Desorber Schematic (Cf. Tables 10 and 11).

Table 10. Tentative Xenon-Plus Iodine Stripper Design by Spray Desorption

(see Fig. 12)

Gas conditions	
Helium flow rate, ft^3/sec	81
Partial pressure HF, atm	0.01
Partial pressure H_2, atm (assumed)	10^{-6}
Upflow velocity in tower, ft/sec (assumed)	2
Gas pipeline velocity, ft/sec (assumed)	20
Liquid conditions	
Flow rate, ft^3/sec (8% primary flow)	10
gpm	4490
Dimensions	
Tower diameter, ft	7.2
Height, ft	~10
Inlet gas pipe diameter, ft	2.3
Degree of separation	
(Anticipated to suffice for 1 transfer unit of xenon and 0.2 transfer unit of iodine separation)	

Table 11. Tentative Iodine Stripper Design by Spray Desorption

(see Fig. 12)

Gas conditions	
Helium carrier gas flow rate, ft^3/sec	93.6
Partial pressure HF, atm	0.01
Partial pressure H_2, atm (assumed)	10^{-6}
Upflow velocity in stripper, ft/sec (assumed)	2
Gas pipeline velocity, ft/sec (assumed)	20
Liquid conditions	
Flow rate, ft^3/sec (0.8% primary flow)	1
gpm	449
Separator dimensions	
Diameter, ft	7.7
Height, ft	~10
Degree of iodine separation	
Anticipated minimum, %	60
Anticipated minimum, number of transfer units	2

3.3 Venturi Stripper for Iodine Removal

Venturi contactors appear to be particularly suited to cases where large gas flows are called for relative to the liquid flow rate. The advantage over spray desorbers lies in the fact that it is the high venturi throat velocity that serves to break up the liquid into small droplets; hence there is less demand for a high-performance spray nozzle. Evidently most experience with venturi contactors is with systems where the gas to liquid volumetric flow ratio is much higher than contemplated for the Xe + I stripper. Hence we will consider this device only for iodine stripping.

Figure 13 shows a flow schematic for iodine stripping by means of a venturi gas-liquid contactor. Note that this is effectively a parallel flow contactor (except in the separator where counterflow conditions exist), hence one should not expect a high degree of separation. Liquid is intensively mixed with stripping gas at the throat of a venturi, followed by a diffuser section to attain as much pressure recovery as possible. Essentially all the liquid holdup will occur in the droplet separator shown conceptually as a large vessel with three stages of mist separation.

The Chemical Engineers' Handbook[17] gives the following empirical equation for estimating the degree of separation that may be attained in a venturi contactor:

$$N = \frac{41.5\ L}{\frac{16050}{V_t} + 1.41\ L^{1.5}}$$

where

N = number of transfer units,

V_t = venturi throat velocity, ft/sec,

L = liquid/gas ratio, gal/1000 ft^3.

If we choose a moderate throat velocity of 200 ft/sec and a Q_g/Q_ℓ of 93.6 appropriate for iodine stripping, Eq. (71) predicts

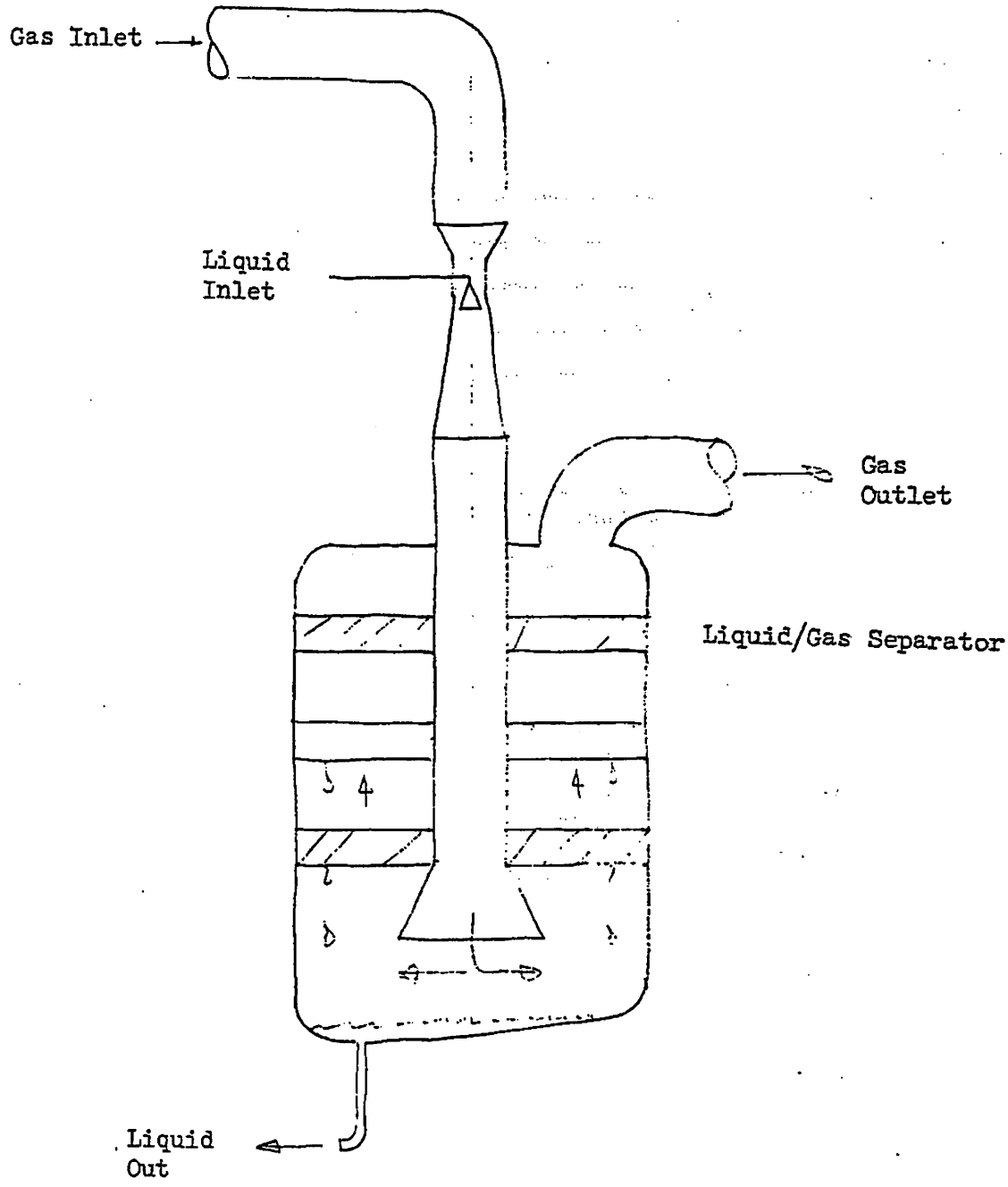

Fig. 13. Venturi Stripper Schematic for Iodine Removal Alone (Cf. Table 12).

$$N = 4.2 \text{ transfer units},$$

which is more than adequate, since only two transfer units are required.

Table 12 lists some pertinent flows and dimensions for the venturi iodine scrubber. Venturi and separator dimensions turn out to be quite reasonable. One potential drawback of this concept is that gas pressure drops across the venturi may become excessive if the liquid is introduced at a low velocity compared with the gas velocity of the throat. High gas pressure drop then occurs due to momentum transfer to the liquid. However, this is not considered to be a serious drawback here since there appears to be adequate opportunity for matching gas and liquid velocities.

Table 12. Tentative Design Conditions for the Venturi Iodine Stripper
(see Fig. 13)

Gas conditions	
Helium carrier gas:	
Partial pressure HF, atm	0.01
Partial pressure H_2, atm (assumed)	10^{-6}
Throat velocity, ft/sec	200
Gas pipeline velocity, ft/sec (assumed)	20
Upflow velocity in separator, ft/sec (assumed)	0.5
Dimensions	
Venturi throat diameter, ft	0.77
Gas pipeline diameter, ft	2.44
Separator tank diameter, ft	15.4
Separator height, ft (approximate)	15
Flow rates	
Stripping gas, ft^3/sec	93.6
Liquid, ft^3/sec (0.8% primary flow)	1
Liquid, gal/min	449
Degree of iodine separation	
Minimum, %	60
Minimum number of transfer units	2
Number of transfer units predicted by Ref. 17	4.3

3.4 The Ramp Flow Stripper

The general features of the ramp stripper are shown in Fig. 14. Molten salt enters at the top where it is distributed across some number of trays (10 shown in the figure) set at a downslope of perhaps 5 to 15°. Liquid flow on the trays is anticipated to be set for approximately 1/4 to 1/2 in. depths with Reynolds numbers in the 10,000 to 50,000 range. This is beyond the range for film flows characteristics of wetted-wall columns.

While the ramp stripper concept is not widely used, neither is it completely unknown. It is closely related to the baffle towers and shower trays noted by Treybal.[18] Additionally, a commercial wet cooling tower recently marketed by Whirlcool is essentially a variant of the ramp contactor concept.

The ramp stripper may be thought of as an adaptation of the wetted-wall contactor to molten salt liquids. Since these do not wet the container material, it is naturally impossible to establish the film-type flow that characterizes wetted-wall columns. In the ramp stripper, the flow is of sufficient depth so that wetting characteristics do not play a role in establishing the flow.

Some desirable features of wetted-wall columns are retained. The ramp stripper, like the wetted-wall column, is particularly suited to high gas and liquid throughputs with low pressure drop. A superior feature is that, as opposed to the wetted-wall column, liquid depths and velocities may be adjusted over wide ranges to suit the designer by alteration of the ramp angle and surface roughness.

It may be shown that the internal eddy conductance in the ramp flow is quite high, and the main resistance to mass transfer exists in the thin surface film at the gas-liquid interface. The success or failure of the concept in large part depends on how well the surface film barrier to mass transfer is penetrated by any of several available devices. In the anticipated Reynolds number range, the liquid surface will be wavy, which, together with the high counterflow gas velocity of approximately 20 ft/sec, is expected to reduce surface resistance to some extent. Wave promoters or mixing baffles may be employed to assist in the penetration of the

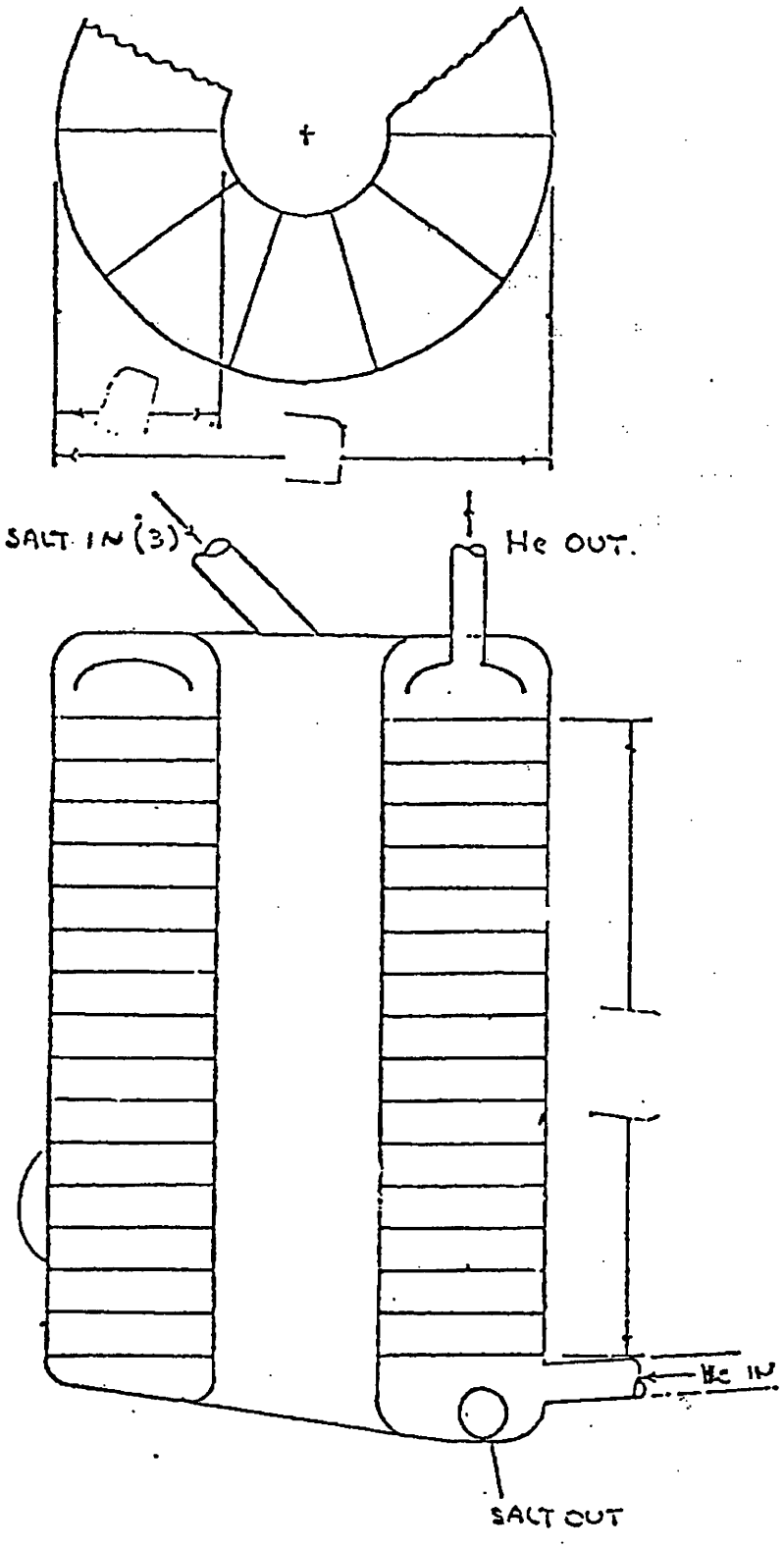

Fig. 14. Ramp Flow Stripper Schematic (Cf. Table 16).

surface film. The commercial cooling tower design by Whirlcool employs small waterfalls spaced about one ft apart down the ramp to enhance mass transfer into the gas phase.

Since this is yet another type of countercurrent contactor, the equations developed in Section 3.1 still apply with the exception that the expression for the height of the transfer unit now takes a different form. It may be shown that the expression for H_L of a ramp contactor is given by

$$H_L = \frac{Q_\ell}{h_m W}, \qquad (72)$$

where h_m is the mass transfer coefficient; W is the total width available for liquid flow. H_L here signifies the distance parallel to the flow incline required to achieve one transfer unit of separation.

3.4.1 Mass Transfer Across a Gas-Liquid Interface

The value of the mass transfer coefficient, which determines the length of a transfer unit along the ramp, is quite uncertain since there evidently have been no mass transfer experiments for this particular situation. Most scalar transport data pertain to enthalpy transport to a smooth wall in a fluid Prandtl number range of 1 to 10.

Table 13 lists four empirical formulae for the mass transfer coefficient together with the conditions for which each equation was developed.[19,20,21] Use of any of these equations for conditions other than they were intended is highly questionable. Note that the first three equations pertain to transfer to a solid wall; only the last applies to transfer across fluid-gas interface.

The fourth column in Table 13 lists the values of h_m computed from each of the listed correlations for some typical liquid flow conditions that may be anticipated; namely, a liquid velocity of 4 ft/sec, depth of 1/4 in., moderately rough ramp surface, and a highly rough gas-liquid interface. It is seen that there exists about two orders of magnitude difference between the lowest and highest values of the mass transfer coefficient. The lowest value is obtained from Eq. (73), which applies to transfer to smooth walls, while the highest value is given by the

Table 13. Mass Transfer Equations and Representative Values

Equation	Formula	Application and Reference	Representative Values[a]	
			Mass Transfer Coefficient (ft/sec)	Length of Transfer Unit (ft)
(73)	$St_m = \frac{f}{Sc^{2/3}}$	Dittus-Boelter; transfer to smooth walls primarily for $1 < Pr, Sc < 10$	0.00010	833
(74)	$St_m = 0.112 \frac{f}{Sc^{3/4}}$	Transfer to smooth walls at high Sc or Pr numbers[b]	0.00017	490
(75)	$St_m = \frac{0.0878\sqrt{f}}{Sc^{0.44}}$	Transfer to rough wall[c] for $1 < Sc, Pr < 7$	0.0013	64
(76)	$St_m = \frac{6.45d}{Sc^{0.5}}$	Xenon sorption and desorption from water film[d] Dimensional equation, d in ft $1000 < Re < 4000$ $300 < Sc < 1500$ $U_g \cong 1/4$ ft/sec	0.012	6.5

[a] Assumed typical conditions: Sc = 1750, f = 0.01, U_ℓ = 4 ft/sec, liquid depth = 0.25 in.

[b] See Ref. 19

[c] See Ref. 20

[d] See Ref. 21

dimensional equation that was found to fit xenon desorption data from water film flow down a rough, vertical surface.

The fourth column of Table 13 lists the length of a transfer unit along the ramp for each case computed from Eq. (72). It may be seen that either of the smooth wall equations, if applicable, would lead to excessively large contactors of this type. If Eq. (76) applies, ramp contactors that carry out the required degree of separation for iodine or xenon stripping can be made quite small in size and liquid holdup.

Equation (76) was derived for an experimental situation that very closely approximates the flow and mass transfer conditions anticipated for the ramp stripper. Xenon and argon were stripped from a water film flowing downward in the device shown in Fig. 15 called a "trombone cooler." Gas flow was upward and set at a velocity of about 1/4 ft/sec. The data are shown in Fig. 16 where the straight line is Eq. (76) of Table 13. Unfortunately, Eq. (37) is a dimensional equation which makes its use even more uncertain outside its known range of applicability. However, the Reynolds and Schmidt number variation in the trombone cooler experiments were not far from assumed conditions on the ramp stripper — the maximum Re was approximately a factor of two lower than assumed ramp conditions while Schmidt numbers are estimated to have reached approximately the value estimated for fuel salt at 1300°F. Unfortunately, all the high Schmidt number data were taken at the lowest Reynolds numbers. In addition, in using Eq. (76) for ramp flows we must extrapolate the liquid depth from its value in the trombone cooler — perhaps 0.05 to 0.1 in. — to the assumed depth on the ramp of 0.25 in. A positive aspect, however, is that no determined effort was made in these experiments to maximize the mass transfer coefficient. Even the gas velocity was quite low — about 1/4 ft/sec compared with about 20 ft/sec anticipated for the ramp. Higher gas velocities may materially help in penetrating the surface film barrier which offers the main resistance to mass transfer.

Some insight to the process of eddy conductance in a liquid flowing down an inclined plane may be obtained from the work of Jepsen[22] who measured eddy diffusivities within water films up to a Reynolds number of 1800. The films were formed by water flow down a ramp of 9° 44 ft incline

DETAILS OF COOLER BOX SIMULATING TROMBONE COOLER BANK

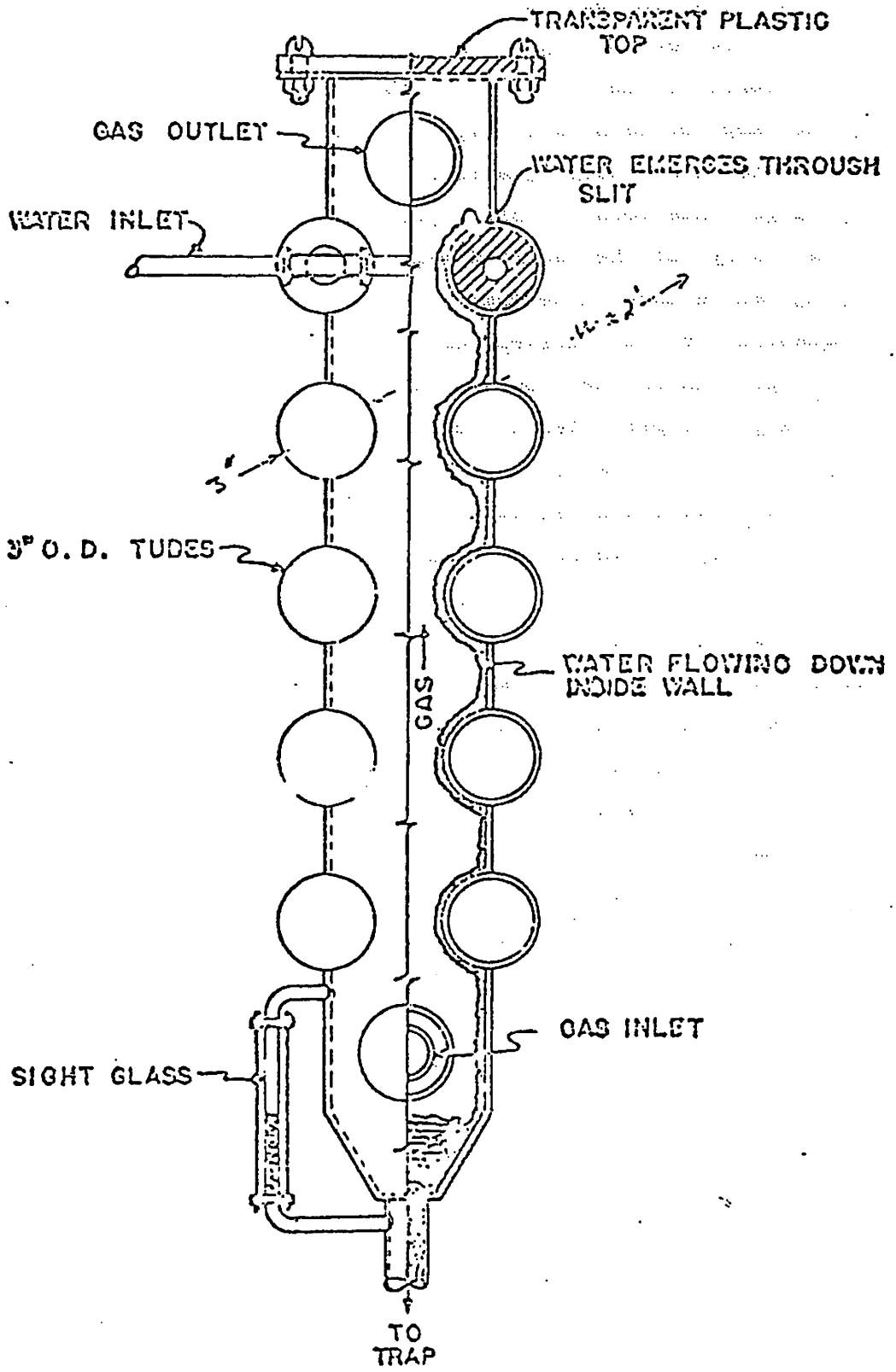

Fig. 15. "Trombone Cooler" for Stripping Xenon from HRT Fuel Solution (Ref. 21)

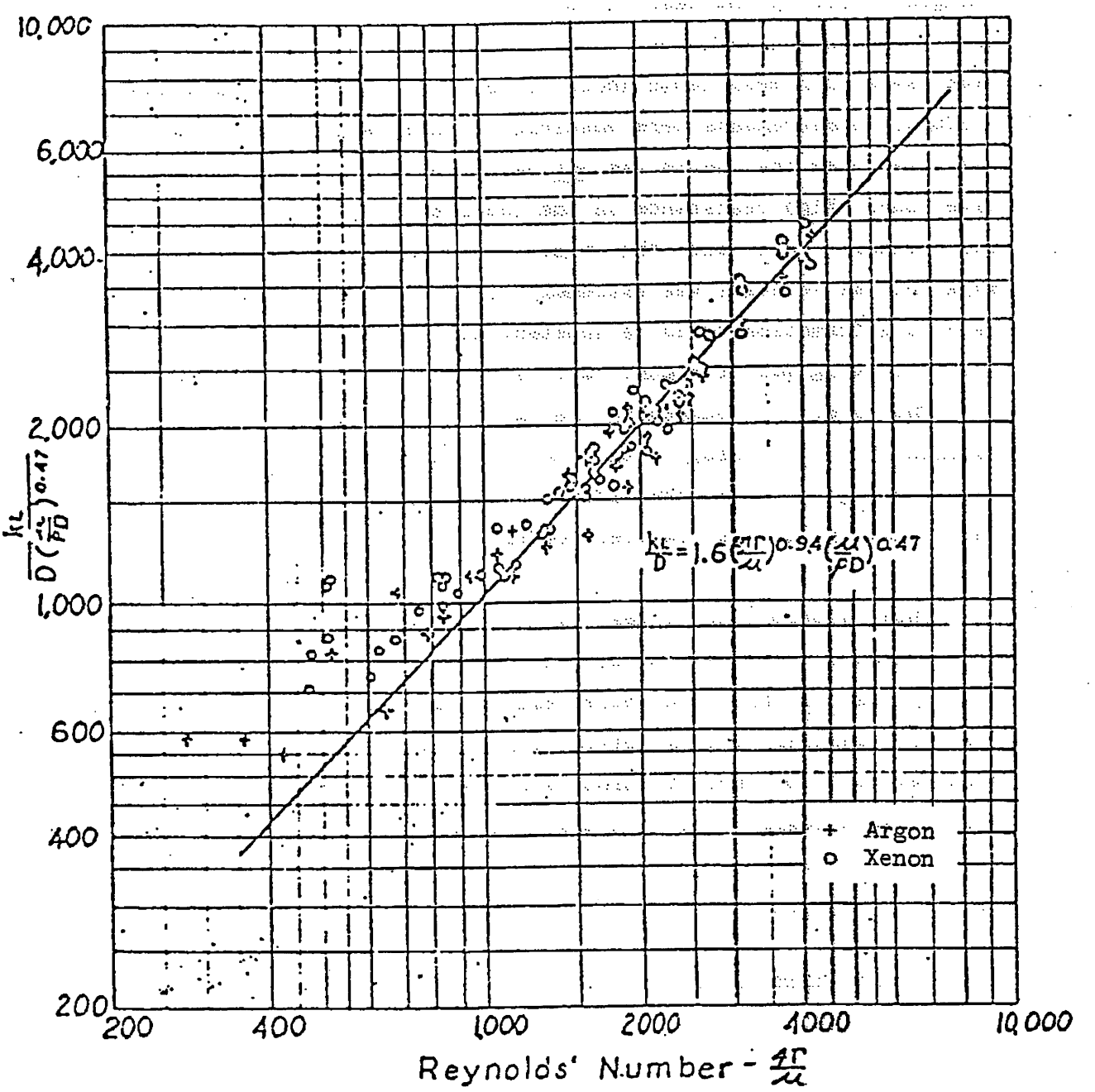

Fig. 16. Correlation of Absorption and Desorption Data for Xenon and Argon from HRT Fuel Solution. (Ref. 21)

with eddy diffusivities being determined optically via refraction index changes caused by the desorption of carbon dioxide. Some of the measurements are summarized in Fig. 17. Most noteworthy is the presence of surface waves with mean depth about 30 to 40% of the film thickness. No diffusion measurements were possible in this range, but visual observation indicated that the liquid was not being intensely mixed in the surface wave zone. High resistance in the interface region was thought to control mass transfer rates into the film. It should be noted, however, that the adjacent gas velocity was extremely low. The degree and effects of surface wave formation could be substantially altered by the traction of counterflowing gas of significant velocity.

The effect of roughening the wall is postulated by the dashed line labeled "b". By analogy with pipe flow data, increased wall roughness should bring the high eddy diffusion zone closer to the bottom surface. Unfortunately no mass transfer coefficients are reported for this experiment.

Thus, appropriate values for h_m in turbulent films flowing down inclined planes are highly uncertain. There have been no measurements on flow systems of this type where deliberate attempts were made to maximize the mass transfer rate by bottom roughening, surface breakers or other such devices. Surface friction caused by counterflowing gas at moderate speed also appears to be an attractive way to diminish mass transfer resistance at the interface. However, neither has this effect been experimentally explored.

3.4.2 Flow Rates on an Inclined Plane

Some characteristics of liquid flow on inclined plane surface are given in Table 14. The given depths and velocities were computed from standard open-channel equations (e.g., Ref. 23) for infinitely long, smooth channels. If the ramp were hydraulically roughened, which would no doubt be desirable, the depth would increase slightly while the velocity would decrease slightly. The Reynolds number, which depends only on the flow rate per unit width, would remain constant. Besides hydraulic roughening, any barriers put on the ramp to augment the mixing process can increase the liquid depth and reduce the velocity to any desired value.

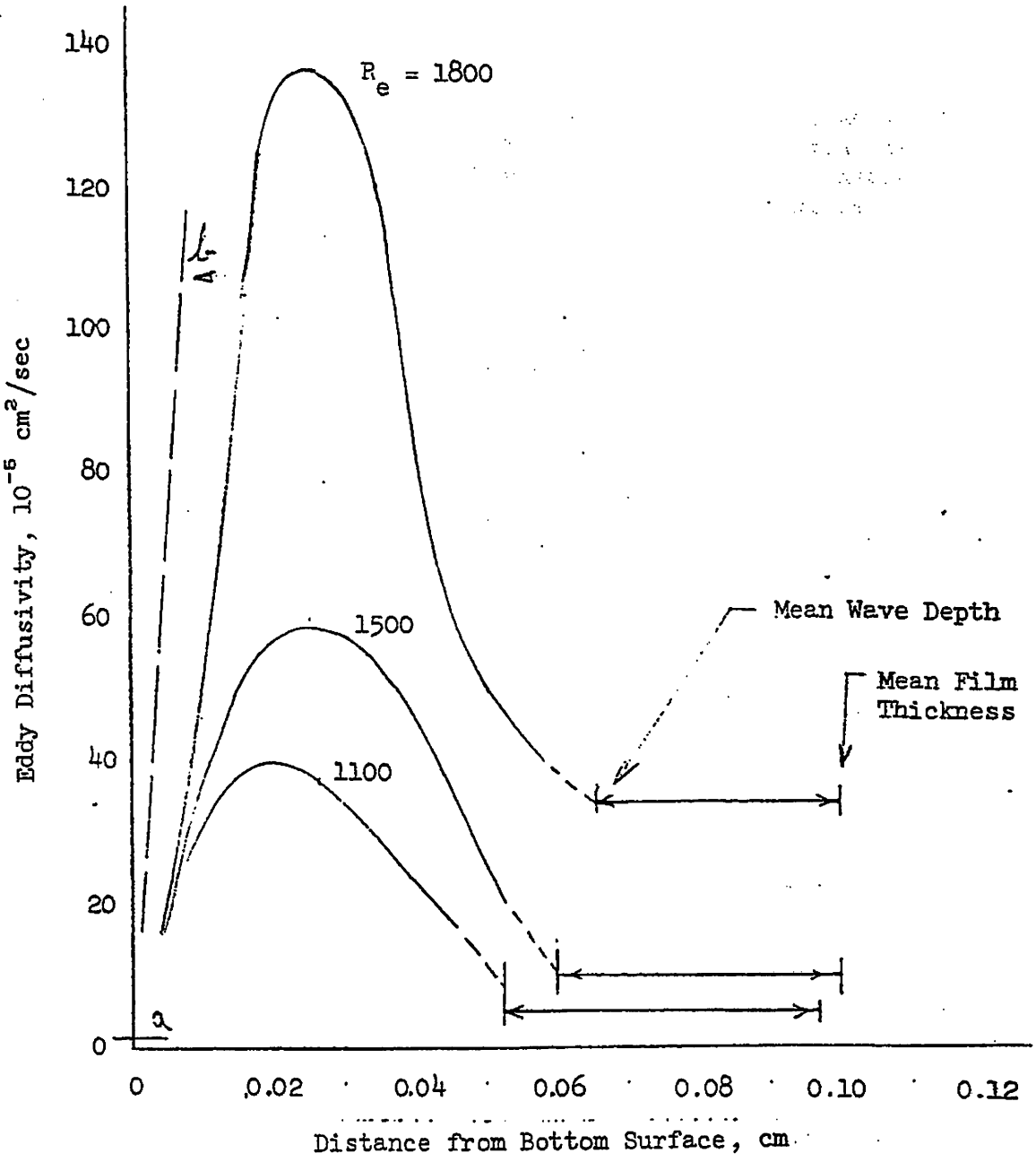

Fig. 17. Eddy Diffusivities and Wave Depths for Water Flow on an Inclined Plane in Still Air.

a - Molecular Diffusivity = 1.5×10^5 cm^2/sec.
b - Postulated Effect of Roughening Surface.

Table 14. Liquid Depths, Velocities and Reynolds Numbers for Long, Smooth Ramps

$$Re_\ell = 4\, Q_\ell\, \rho / W \mu$$

Flow Rate Per Unit Width (ft^3/sec-ft)	Re_ℓ	Ramp Angle (°)	Depth on Long, Smooth Surface (ft)	Liquid Velocity (ft/sec)
0.375	61,000	5	0.058	6.5
		10	0.047	8.0
		15	0.042	9.0
0.25	41,000	5	0.045	5.5
		10	0.037	6.8[a]
		15	0.032	7.7
0.19	31,000	5	0.038	4.9
		10	0.031	6.1
		15	0.027	6.9
0.15	24,000	5	0.033	4.5
		10	0.027	5.6[b]
		15	0.024	6.3

[a]Selected for Xe + I stripper.

[b]Selected for iodine stripper.

The ramp angle and flow per unit widths selected for the Xe + I stripper case and for iodine stripping alone are indicated by a and b in Table 14. These selections ultimately would be made by an optimization procedure; however, a brief survey indicated these to be reasonable choices.

3.4.3 Ramp Stripper for Xe + I Removal

Some design specifications for a combined Xe + I stripper based on the ramp concept are listed in Table 15. It is again emphasized that these size requirements are speculative; the main purpose for listing them here is to offer some idea of the sizes, flows, and liquid holdups that may be expected.

No mass transfer data are available for flows of this type. It was felt, however, that designs based on Eq. (75), which applies to transfer

Table 15. Combined Xe + I Ramp Stripper Conservative and Optimistic Designs

Flow conditions from Case a, Table 14

Design conditions		
Fuel salt flow rate, ft^3/sec (8% primary flow)		10
Stripping gas flow rate, ft^3/sec		81
Xenon removal efficiency, % (1 transfer unit)		63
Iodine removal efficiency, % (0.2 transfer unit, not controlling)		6
HF partial pressure, atm		0.01
	Conservative Design Eq. (75)	Optimistic Design Eq. (76)
Ramp characteristics		
Slope, deg	10	10
Total width, ft	40	40
Length, ft (1 transfer unit)	113	6.4
Liquid velocity, ft/sec	6.8	6.8
Liquid depth, in.	0.44	0.44
Liquid Reynolds number	41,000	41,000
Liquid holdup, ft^3	167	9.5
Mass transfer coefficient, ft/sec	0.0022	0.039

to rough walls, and Eq. (76) for xenon stripping from water films, should bracket the range of possibilities. Note that somewhere between 10 and 170 ft^3 of liquid holdup is required for Xe + I stripping from ramp flow to counterflow stripping gas.

3.4.4 Ramp Stripper for Iodine Removal

Table 16 lists some speculative design specifications for an iodine stripper based on the ramp contactor concept. Note that the anticipated liquid holdup ranges between 2 to 30 ft^3.

Table 16. Iodine Stripper, Ramp Concept
Conservative and Optimistic Designs

Flow conditions from Case b, Table 14

Design conditions		
Fuel salt flow rate, ft^3/sec (1% primary flow)		1
Stripping gas flow rate, ft^3/sec		93.6
Iodine removal efficiency, % (2 transfer units)		60
HF partial pressure, atm		0.01
	Conservative Design Eq. (75)	Optimistic Design Eq. (76)
Ramp characteristics		
Slope, deg	10	10
Total width, ft	6.7	6.7
Length (2 transfer units)	163	12.9
Liquid velocity, ft/sec	5.6	5.6
Liquid depth, in.	0.32	0.32
Liquid Reynolds number	24,000	24,000
Liquid holdup, ft^3	29	2.3
Mass transfer coefficient, ft/sec	0.0018	0.023

3.5 Packed Column Strippers

Packed columns are one of the more common means for effecting gas-liquid contact, however, they have some inherent drawbacks as potential iodine strippers. First, fuel salt does not wet the packing material, hence the surface area for interphase contact is substantially less than the area provided by the packing. This appears to be reflected in the rather low effective mass transfer coefficients reported by Lindauer.[24,25] This type of flow through packing has not been visually observed in gas-liquid systems, but has been studied in liquid-liquid extraction systems where the situation arises far more frequently. In liquid-liquid packed column flow, when the heavy phase is dispersed and nonwetting, it is observed that the heavy phase showers downward as discrete droplets when the packing material exceeds some critical size, d_{pc}. Watson,[26] for the mercury-water system, gives

$$d_{pc} = 3\sqrt{\frac{\sigma}{\Delta\rho g}}, \qquad (72)$$

where σ is the interphase surface tension, and $\Delta\rho$ the density difference between phases. For fuel salt-helium, Eq. (72) predicts a critical packing size of 1/4 in.

Nonwetting flow through packing of size less than d_{pc} yields erratic results because the flow tends to trickle through the packing in continuous streams instead of by discrete droplets. Much lower values for effective k_L result because far less interphase surface area is exposed.

A second possible drawback of packed columns as iodine strippers is that they may require high gas pressure drop to force through the large volumes of gas that are required, especially when the packing size is small.

In attempting to estimate unit sizes and liquid holdups for packed-column iodine and Xe + I strippers, the following assumptions and estimates were used.

1. An effective value for k_L of 0.02 ft/hr was selected which may appear to be rather optimistic since Lindauer[24,25] reports values in the range 0.001 to 0.03 ft/hr. This relatively high value was selected because the reported data pertain to columns only 1 in. in diameter where no doubt a large fraction of the liquid flows directly down the wall of the column. In addition, the packing size was 1/4 in. which may be below the critical packing size.

2. In the absence of any general correlation for liquid holdup for this case, we used the data of Lindauer[27] for molten salt flow in a packed bed of Raschig rings of 1/4 in. diam by 1/32-in. wall thickness. For this case it was found that

$$\epsilon_\ell = 0.04 + 2.8\, U_\ell \qquad (73)$$

where ϵ_ℓ is the liquid fraction of the free volume and U_ℓ the superficial liquid velocity in ft/sec. ϵ_ℓ was found to reach as high as 0.15 after which the flooding point was soon reached, and was observed to be insensitive with gas flow variation.

3. The gas pressure drop as a function of gas and liquid flow rate and packing size was estimated using correlations that apply to wetted packing. This is in error to some degree, but there appears to be no other recourse at this time. The summary presented by Coulson and Richardson[28] was used.

3.5.1 Xe + I Stripping by Packed Column

It may readily be seen that packed columns for Xe + I stripping will be excessively large based on information that is available at this time. For example, if 3/8-in. Berl saddles are used that yield 190 ft^2 surface area/ft^3 of column, then for a 15-ft-diam column, Eq. (60) yields,

$$H_L = 53 \text{ ft} ,$$

assuming a value for k_L of 0.02 ft/hr. Since one transfer unit of separation is required for this case, it is difficult to see how a packed column can be considered unless new data show that k_L may be significantly larger in larger diameter columns and larger sized packing.

3.5.2 Packed Column Iodine Stripper

Table 17 lists some pertinent design characteristics of a packed column used for iodine stripping. The column is large, but perhaps within the realm of possibility. Again the main factor in causing the column to be large is the low value for the effective mass transfer coefficient. If k_L can be brought up to the range of 0.1 ft/hr, packed columns would definitely be in the running for use in iodine stripping. Note that even for the relatively large column, described by Table 17, the liquid holdup is a moderate 79 ft^3.

Table 17. Packed Column Iodine Stripper

Assumed conditions	
Fuel salt flow rate, ft^3/sec	1
Stripping gas flow rate, ft^3/sec	93.6
Required iodine separation, % (2 transfer units)	60
HF partial pressure, atm	0.01
k_L, ft/hr	0.02
Column characteristics	
Packing material	3/8-in. Berl saddles
Surface area/ft^3 column, ft^2/ft^3	190
Free volume, %	65
H_L, ft	8.3
Column diameter, ft	12
Column height, ft	16.6
Superficial liquid velocity, ft/sec	0.0088
Superficial gas velocity, ft/sec	0.83
Liquid holdup, ft^3	79
Gas pressure drop, in. H_2O	0.15

Nomenclature for Side-Stream Processing Section

A	Cross-sectional area of packed column, ft^2
A_b	Total bubble surface area in sparger, cm^2
a	Packing surface area per unit volume, ft^{-1}
C	Constant defined by Eq. (18), sec^{-1}
d_b	Bubble diameter, cm
d_p	Packing size, in.
d_{pc}	Critical packing size, in.
D	Diffusion coefficient, cm^2/sec
h_m	Mass transfer coefficient, ft/sec
H_L	Height of a transfer unit, ft
H_{LR}	Length of a transfer unit along ramp stripper, ft
K'	Equilibrium constant defined by Eq. (9), $cm^3/g\text{-mole}$
K_{HF}, K_{HI}	Solubility coefficients, $g\text{-mole}/cm^3\text{-atm}$
K_{eff}	Effective solubility of I^-, $g\text{-mole}/cm^3\text{-atm}$
k_L	Mass transfer coefficient in packed column, ft/hr
m	Slope of $\ell n[I^-]$ vs n_{HF}
n_{HF}	g-moles HF passed
N_L	Number of transfer units
P_{HF}, P_{HI}	Partial pressures, atm
Q	Volume flow rate of sparge gas in laboratory experiment, cm^3/sec
$Q_l Q_g$	Liquid and gas flow rates in contactor, ft^3/sec
Q_1	Equilibrium quotient defined by Eq. (24), kg/g-mole
Q_0	Minimum stripping gas flow required for efficiency, η
Q_p	Side-stream process flow rate, ft^3/sec
R	Gas constant, $cm^3\text{-atm}/g\text{-mole-}°K$
Re_b	Bubble Reynolds number
r	Dimensionless removal rate defined in Eq. (1)
Sc	Schmidt number = ν/D
Sh	Sherwood number = $h_m d_b/D$
U_L	Liquid velocity on ramp, ft/sec
u_t	Terminal rise velocity of bubble, cm/sec
V	Volume of melt in laboratory experiment, cm^3

V	Loop volume, ft^3
W	Width of ramp contactor, ft
w	Weight of melt in laboratory experiment, kg
X	Mole fraction
Y_{Xe}, Y_I	Fractions of mass-135 yield that is directly Xe and I
Z	Column height, ft
Z_R	Ramp length, ft
$[\ ]$	Concentration, $g\text{-mole}/cm^3$
$(\ )$	Activity
ϵ	Void fraction
$\Delta\rho$	Density difference between phases, g/cm^3
μ	Viscosity, g/cm-sec
ν	Kinematic viscosity, cm^2/sec
σ	Surface tension, $g\text{-}cm/sec^2$

Subscripts

G	Pertains to graphite pores
g	Pertains to gas
ℓ	Pertains to liquid
2	Pertains to rich end of stripper
1	Pertains to lean end of stripper
0	Reference or initial value

Superscripts

*	Pertains to liquid surface

REFERENCES

1. C. E. Bamberger and C. F. Baes, Jr., Removal of Iodide from L_2B Melts by HF-H_2 Sparging, p. 127, MSR Progr. Semiann. Progr. Rept. Aug. 31, 1965, ORNL-3872, Oak Ridge National Laboratory.

2. B. F. Freasier, C. F. Baes, Jr., and H. H. Stone, Removal of Iodine from LiF-BeF_2 Melts, p. 38, Reactor Chem. Div. Ann. Progr. Rept. Dec. 31, 1965, ORNL-3913, Oak Ridge National Laboratory.

3. C. E. Bamberger and C. F. Baes, Jr., Removal of Iodide from L_2B Melts, p. 32, Reactor Chem. Div. Ann. Progr. Rept. Dec. 31, 1966, ORNL-4076, Oak Ridge National Laboratory.

4. Letter from C. F. Baes, Oak Ridge National Laboratory, to R. P. Wichner, Oak Ridge National Laboratory, Aug. 2, 1971, Subject: Further Comment on Iodine Removal by HF Sparging.

5. J. R. Fair, Designing Gas Sparged Reactors, Chem. Eng., 74(14): 67–74 (1967).

6. R. W. Schaftlein and T. W. F. Russel, Two-Phase Reactor Design, Ind. Eng. Chem., 60: 13–27 (1968).

7. O. Kubachewski et al., Metallurgical Thermochemestry, 4th ed., Table D, Pergamon Press, Oxford.

8. JANAF Thermochemical Tables, 2nd ed., Dow Chemical Co., June 1971.

9. F. J. Smith et al., Liquid-Vapor Equilibria in LiF-BeF_2 and LiF-BeF_2-ThF_4 Systems, Table 2, ORNL-4415, Oak Ridge National Laboratory.

10. B. F. Hitch and C. F. Baes, Inorg. Chem., 8: 201 (1969).

11. C. F. Baes, Estimation of Activity Coefficient in LiF-BeF_2-ThF_4 Melts, p. 152, ORNL-4548, Oak Ridge National Laboratory.

12. J. M. Coulson and J. F. Richardson, Chemical Engineering, vol. II, 2nd ed., p. 452, Pergamon Press, Oxford, 1966.

13. R. M. Griffith, Chem. Eng. Sci., 12: 198 (1960)

14. Chemical Engineers' Handbook, J. H. Perry (ed.), 4th ed., Fig. 18-107a,b, McGraw-Hill, New York.

15. S. M. Rajan and W. J. Heideger, Drop Formation Mass Transfer, pp. 202–206, AIChE J., January 1971.

16. D. M. Eissenberg and I. Spiewak, Vacuum Deaerators for Distillation Plants, paper presented at the OSW Symposium on Feed Treatment for Distillation Plants, April 6–7, 1971, Tulsa.

17. Chemical Engineers' Handbook, J. H. Perry (ed.), 4th ed., pp. 18–56, McGraw-Hill, New York.

18. R. E. Treybal, Mass-Transfer Operations, 2nd ed. p. 152, McGraw-Hill, New York, 1968.

19. R. G. Deissler, Analysis of Turbulent Heat Transfer, Mass Transfer and Friction on Smooth Tubes at High Pr and Sc Numbers, NASA, Rept. 12:0.

20. D. F. Dipprey and R. H. Sabersky, Heat and Momentum Transfer in Smooth and Rough Tubes at Various Pr, J. Heat Mass Trans., 6: 329–353 (1963).

21. G. W. Haldeman et al., Sorption and Desorption of A and Xe in a Trombone Cooler, Mont-154, 1946.

22. J. C. Jepsen et al., The Effect of Wave-Induced Turbulence on the Rate of Absorption of Gases in Falling Liquid Films, AIChE J., 12: 186–192 (1966).

23. S. Whitaker, Introduction to Fluid Mechanics, p. 353, Prentice-Hall, New York, 1968.

24. R. B. Lindauer, p. 269, MSR Progr. Semiann. Progr. Rept., Feb. 28, 1971, ORNL-4676, Oak Ridge National Laboratory.

25. R. B. Lindauer, p. 47, MSR Monthly Rept., Oct. 29, 1971, Oak Ridge National Laboratory.

26. J. S. Watson, p. 29, CTD Ann. Progr. Rept., March 1971, ORNL-4682, Oak Ridge National Laboratory.

27. R. B. Lindauer, MSR Monthly Report, Period Ending Jan. 30, 1972, Oak Ridge National Laboratory.

28. J. M. Coulson and J. F. Richardson, Chemical Engineering, vol. II, 2nd ed., Chap. 1, Pergamon Press, New York, 1968.